

Summer of Science 2020

High Energy Astrophysics

Manan Seth
Mentor: Joy Sanghvi

Contents

0.1	Introduction	ii
1	Prerequisites	1
1.1	Special Theory of Relativity	1
1.1.1	Need for Relativity and Einstein's postulates	1
1.1.2	The Theory	1
1.1.3	Some Useful Results	2
2	Cosmic Rays	4
2.1	Discovery and Detection	4
2.2	Possible Sources	5
2.3	Ultra High Energy Cosmic Rays	5
3	Stellar Astrophysics	7
3.1	Introduction	7
3.2	Equations of Stellar Structure	8
3.2.1	Hydrostatic Support	8
3.2.2	Equation of Energy Generation	9
3.2.3	Equation of Radiative Transport	10
3.3	Stellar Structure	10
3.4	Stellar Evolution	11
3.4.1	Hayashi Track	11
3.4.2	High Mass Stars	11
3.4.3	Low Mass Stars	12
3.5	Mass Loss	12
3.5.1	P-Cygni Profiles and Wolf Rayet Stars	12
4	Galaxies	14
4.1	The Hubble Sequence	14
4.2	Milky Way	14
4.2.1	Gas in the Milky Way	15
4.3	Other Galaxies	15
4.3.1	Galaxies in the Expanding Universe	15
4.4	Galaxy Clusters	16
5	Important Physical Processes	17
5.1	Nuclear Interactions	17
5.1.1	Introduction	17
5.1.2	Spallation cross-sections	18
5.1.3	Nuclear Emission Lines	19
5.2	Ionisation Losses	20
5.2.1	Non Relativistic Treatment	20
5.2.2	The Relativistic Case	22

5.2.3	Ionisation Losses of Electrons	23
5.3	Radiation of Accelerated Charged Particles	23
5.3.1	Relativistic Invariants	24
5.3.2	The Radiation of Accelerated Charged Particle	24
5.3.3	Bremsstrahlung	28
5.4	Synchrotron Radiation	33
5.4.1	Dynamics of Charged Particles in Uniform Magnetic Fields	33
5.4.2	Synchrotron Total Energy Loss Rate	34
5.4.3	Non-relativistic Gyroradiation and Cyclotron Radiation	35
5.5	Interactions of High Energy Photons	36
5.5.1	Photoelectric Absorption	36
5.5.2	Thomson and Compton Scattering	36
6	High Energy Astrophysics	39
6.1	Interstellar Gas	39
6.1.1	Neutral Interstellar Gas	39
6.1.2	Ionised Interstellar Gas	40
6.1.3	Overall Picture of Interstellar Gas	40
6.2	Dead Stars	41
6.2.1	Sirius B	42
6.2.2	White Dwarfs	42
6.2.3	Dwarf Novae	43
6.2.4	Accretion Disks	45
6.2.5	Classical Novae and the Chandrasekhar Limit	46
6.2.6	Supernovae	48
6.2.7	Neutron Stars	51
6.2.8	Black Holes	53
6.3	Active Galactic Nuclei	55

0.1 Introduction

High Energy Astrophysics is a field of study which deals with understanding and explaining several phenomena involving high energy cosmic rays, the death of massive stars and other explosions in the universe and various sources of electromagnetic radiation observed in these cases.

In the past two months I have attempted to study these phenomena and many related topics which I found interesting and helpful to understand said phenomena. In this report I have summarised the concepts I learnt, starting with the basics of special relativity and astronomy, moving over to the basics of stellar and galactic evolution, followed by various physical processes which produce cosmic rays and electromagnetic radiation, finally ending with various high energy events in our solar system dealing with white dwarfs, supernovae, neutron stars, black holes and more.

Chapter 1

Prerequisites

1.1 Special Theory of Relativity

Considering many high energy phenomena involve relativistic speeds, the Special Theory of Relativity has been covered as a prerequisite in enough depth to understand time dilation, length contraction, Doppler shift, energy and beaming in the relativistic view.

1.1.1 Need for Relativity and Einstein's postulates

For a long time, the Galileian view of relativity was considered to be the complete picture of viewing the world from different reference frames. This was not a big issue for transformations between reference frames at non relativistic speeds with respect to each other. Yet in the Michelson–Morley experiment in 1887 which tried to find the velocity of Earth moving through the ether (a proposal of a non-interacting medium in which light waves were formed), the speed of earth relative to the ether was found to be exactly zero in all directions and essentially non accelerating frames of reference, indicating a constant speed of light in all frames of reference.

This experiment disproved the validity of Galileian transformations in relativistic scenarios. Thus using the constancy of speed of light as a postulate, the second and only other postulate being that the laws of Physics are same in all inertial reference frames, Special Theory of Relativity was derived.

1.1.2 The Theory

This started with the Lorentz Transformations. Without loss of generality, two reference frames S and S' are assumed where the latter is moving with a velocity of u in the positive x direction when viewed from the former. Then the Lorentz Transformation equations derived are:

$$\begin{aligned}x' &= \frac{x - ut}{\sqrt{1 - u^2/c^2}} \\y' &= y \\z' &= z \\t' &= \frac{t - ux/c^2}{\sqrt{1 - u^2/c^2}}\end{aligned}$$

Using these equations, it is easy to observe the effects of time dilation

$$\Delta t_{moving} = \frac{\Delta t_{rest}}{\sqrt{1 - u^2/c^2}}$$

and length contraction

$$L_{\text{moving}} = L_{\text{rest}} \sqrt{1 - u^2/c^2}$$

The formulae of energy and momentum in relativistic frames are also affected. However, the derivations are too involved for a prerequisite topic.

Total relativistic energy is γmc^2 and total kinetic energy is $mc^2(\gamma - 1)$. Here γ is the Lorentz factor:

$$\gamma = \frac{1}{\sqrt{1 - v^2/c^2}}$$

Similarly, relativistic momentum is given by $\gamma m\mathbf{v}$.

1.1.3 Some Useful Results

If a source of light is moving at relativistic speeds, it is important to consider the relativistic Doppler shift. It is a qualitatively different to the Doppler shift of sound waves as it involves no medium and the speed of light is constant in all reference frames.

Example 1:

To derive this, let's consider a distant light source which emits a light signal at a time interval of Δt_{rest} as observed from the reference frame of the source. Let this be moving relative to the observer with a velocity \mathbf{u} , as shown in Figure 1.

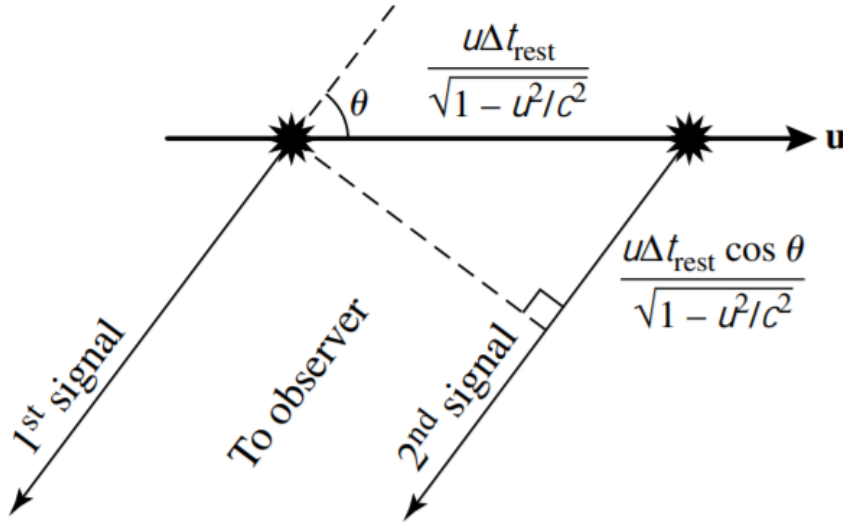


Figure 1.1: Finding the Doppler Shift. [1]

Here, both the effects of time dilation and different distances travelled by light need to be considered. The observed time interval from the observer's frame will be $\Delta t_{\text{obs}} = \Delta t_{\text{rest}} / \sqrt{1 - u^2/c^2}$. However, in this time the light source has moved a distance of $u\Delta t_{\text{rest}} \cos \theta / \sqrt{1 - u^2/c^2}$ away from the observer. Thus the total time interval observed will be

$$\text{Total}\Delta t = \Delta t_{\text{obs}} + (u\Delta t_{\text{rest}} \cos \theta / \sqrt{1 - u^2/c^2})/c$$

Taking $\nu = 1/\Delta t$,

$$\nu_{\text{obs}} = \nu_{\text{rest}} \left(\frac{\sqrt{1 - u^2/c^2}}{1 + (u \cos \theta)/c} \right) = \nu_{\text{rest}} \left(\frac{\sqrt{1 - u^2/c^2}}{1 + v_{\text{radial}}/c} \right)$$

Another relevant concept that can be understood almost entirely by STR is relativistic beaming. When a source of light is moving towards an observer at relativistic speeds, the latter observes a higher intensity of light than would be expected from a light source at rest.

Example 2:

Let a light source be at rest in S' and emit light equally in all directions. Thus in frame S' , half of it is along the positive x' direction. However in a frame where the light source is moving along the positive x direction at a relativistic speed u , the scenario changes.

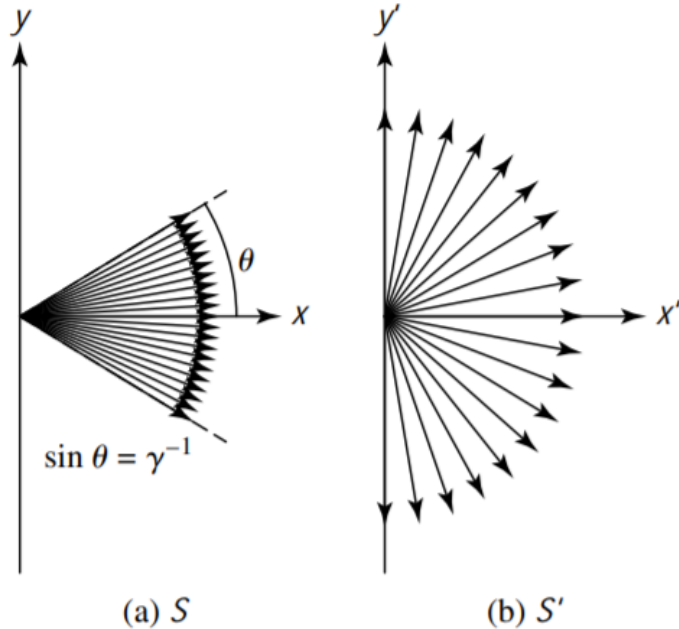


Figure 1.2: Relativistic Beaming or Relativistic Headlight Effect. [1]

Consider the light ray which is moving in positive y' axis direction as observed from frame S' . Then its velocity components will be $v_x = 0$, $v_y = c$ and $v_z = 0$. Using Lorentz velocity transformations (obtained by taking the derivatives of x' , y' and z' with respect to dt') in the opposite direction (converting from S' to S which can be replacing primed terms by unprimed terms and replacing u with $-u$):

$$\begin{aligned} v_x &= \frac{v_x + u}{1 + uv'_x/c^2} = u \\ v_y &= \frac{v'_y \sqrt{1 - u^2/c^2}}{1 + uv'_x/c^2} = c\sqrt{1 - u^2/c^2} \\ v_z &= \frac{v'_z \sqrt{1 - u^2/c^2}}{1 + uv'_x/c^2} = 0 \end{aligned}$$

As measured in S , this ray of light is not moving towards y but also has some positive x component. This shows that more than half the light goes in the positive x direction.

Chapter 2

Cosmic Rays

For any kind of astronomy, observations are important. However, light based observations can only show us so much and it is helpful to look at other sources such as cosmic rays. These are very high energy particles such as protons or atomic nuclei with non terrestrial origins.

2.1 Discovery and Detection

Cosmic rays were first detected around the year 1900 when electroscopes got discharged in the dark even when kept well away from natural radioactive sources. The major breakthrough came in 1912 and 1913 when Hess and Kolhorster studied the ionisation of the atmosphere with altitude and found that it started to increase with height above 1.5 km from the sea level. This confirmed that the source of this ionisation came from above the earth's atmosphere. Finally in 1929, Skobeltzyn detected them directly in a cloud chamber, the Geiger-Muller detector was created which can detect individual cosmic rays and their exact arrival time precisely and Bothe and Kolhorster introduced the concept of coincidence counting, a method used even today to reduce background noise events.

Most cosmic rays do not reach the ground as they interact with the molecules in the air and create a shower of secondary and tertiary particles, called a cosmic ray shower. These can be detected at ground level.

The primary source particles have energies generally exceeding 10^{15} eV. The particles reaching sea level have energies around $10^9 - 10^{10}$ eV. The cosmic ray shower consists of hadronic, muonic and electromagnetic parts. The hadronic component starts with charged (both positive and negative) and neutral pions in the ratio 2:1. However, these quickly decay into further particles like photons, e^+e^- pairs and converts some energy to form muons and thus does not reach the ground. For ultra high energy cosmic rays (UHECR, typically $E \geq 10^{17}$ eV) the muons typically reach the ground and can be detected via scintillation counters or water tanks where their Cherenkov radiation can be detected. The electromagnetic parts can be detected normally based on their energy ranges.

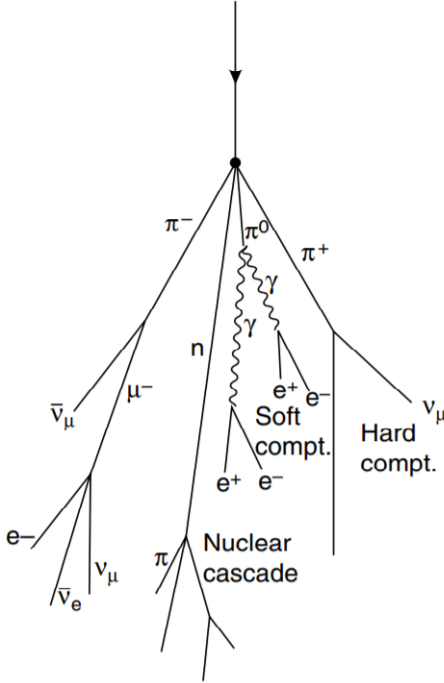


Figure 2.1: Development of a cosmic ray shower showing Soft Electromagnetic, hard penetrating muon and hadronic components. [2]

2.2 Possible Sources

Cosmic rays of energies $\leq 10^{15}$ eV almost certainly originate within our galaxy. The rate of one supernova every $30 - 100$ years in the milky way is enough to explain the observed 5×10^{40} erg s $^{-1}$ of power observed in these cosmic rays, after considering that 1% of the energy is fuels the cosmic rays. The non uniformity of magnetic fields throughout the galaxy gives them their isotropic nature of their apparent direction of origin. Most of the higher energy particles probably have extra galactic origins such as gamma ray bursts or active galactic nuclei (These topics will be studied in depth in the full report).

2.3 Ultra High Energy Cosmic Rays

UHECRs with energies above $\approx 10^{20}$ eV are expected to not last long though as at this energy, accounting for relativistic effects, they can interact with the Cosmic Microwave Background (CMB) photons and lose their energy to them.

Upon interaction protons may form neutral pions and lower energy protons or positive pions and neutrons. This might seem impossible at first - after all the mass of a pion is ≈ 140 MeV/c 2 while CMB photons have energies of only $\approx 10^{-3}$ eV. Yet they interact because of the large Lorentz factor of the protons of $\gamma_p \approx 10^{20}/m_pc^2 \approx 10^{11}$ which makes CMB photons appear to have an energy of $10^{-3} \times 10^{11} \approx 100$ MeV. Since the CMB follows a blackbody distribution, there are sufficient number of photons with the required energy.

To see just how far these can travel without interacting with the CMB, we need to find their mean free path. Their mean free path λ_p is defined as follows:

$$\lambda_p \approx \frac{1}{\sigma_{p\gamma} n_{\gamma th}}$$

Here n_γ is the average spatial density of photons and $n_{\gamma th}$ is density of photons above threshold energy (this value is slightly lower than n_γ). $\sigma_{p\gamma}$ is the probability of interaction per encounter. Using the values $n_{\gamma th} \approx 20 \text{ cm}^{-3}$ and $\sigma \approx 5 \times 10^{28} \text{ cm}^2$, we get:

$$\lambda_p \approx 50 \text{ Mpc}$$

Chapter 3

Stellar Astrophysics

3.1 Introduction

The study of stellar formation and evolution is an integral part of astrophysics. The later stages of some of the most massive stars are the source of many high energy phenomena and hence it is important to get an insight into these topics.

Starting off with some definitions, the effective temperature T_{eff} of a star is defined as the temperature of a blackbody of same radius and luminosity as the star in question. This needs to be defined as despite being some of the nearest examples to perfect blackbodies in the universe, stars have deep absorption lines across many wavelengths which leads them away from true blackbody nature.

Next it is important to know the magnitude system used in astronomy. The apparent magnitude m of a star is measured in a logarithmic scale where an increase of magnitude by 1 indicates a decrease in brightness by a factor of 2.512. The reason for this system is historical. Thus, the formula for apparent magnitude is

$$m = -2.512 \log \frac{I}{I_o}$$

Here I_o is the reference magnitude star and the star Vega was selected for this due to it being visible throughout the year and having a consistent brightness.

We can also define a quantity called absolute magnitude M which denotes the apparent magnitude of a star when viewed from a distance of 10 parsecs from the observer. Thus its formula is given by

$$m = M + 5 \log \frac{d}{10}$$

Here d is the distance to the star in parsecs.

Further it is important to know a bit about Hertzsprung Russel diagrams or HR diagrams which are simple to plot and can help us derive large amounts of data and represent it pictorially. These are graphs which plot the Luminosity of stars (or galaxies) against their Temperature. Although it is sometimes easier to directly plot a colour magnitude diagram instead where colour is defined as the difference in magnitudes in two bands. HR diagrams can be used to find out information such as the age and distance to a cluster and the distribution of different kinds of stars.

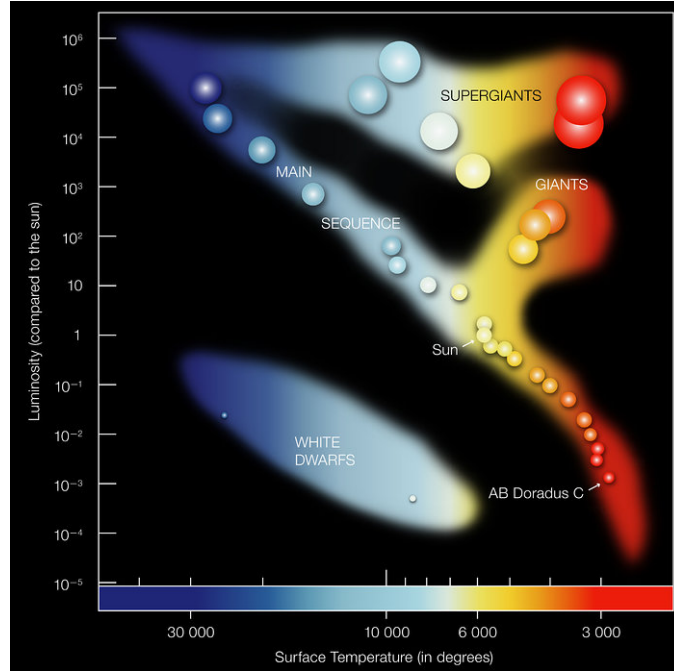


Figure 3.1: An animated HR Diagram. [3]

Finally it is important to note that it is convenient to use some units in the terms of solar units. Some examples of these are the solar mass $M_o = 2 \times 10^{30}$ kg and solar luminosity $L_o = 4 \times 10^{26}$ W.

3.2 Equations of Stellar Structure

There are four equations of stellar structure (along with an equation of state, not covered here) which describe the structure and evolution of the star.

3.2.1 Hydrostatic Support

Let $M(r)$ be the total mass enclosed in r , $\rho(r)$ be density. M_T be total stellar mass and R be the radius.

$$F_{gr} = \frac{GMm}{r^2} = \frac{GM\rho(r) dA dr}{r^2} \quad (3.1)$$

$$F_p = dA[p(r) - p(r + dr)] = -dA dr \frac{dp}{dr} \quad (3.2)$$

Here F_{gr} is inward force due to gravity, F_p is outward pressure force and $p(r)$ denotes pressure at radius r from the centre.

Mass Conservation

Using $dM = M(r + dr) - M(r) = 4\pi r^2 \rho(r) dr$ Using the equations (3.1) and (3.2):

$$\frac{dp}{dr} = -\frac{GM\rho}{r^2} \frac{dM}{dr} = 4\pi r^2 \rho$$

These give the following result

$$\frac{dp}{dM} = -\frac{GM}{4\pi r^4} \quad (3.3)$$

Integrating,

$$-\int_0^{M_T} \frac{dp}{dM} = p_{\text{centre}} - p_{\text{surface}} = \int_0^{M_T} \frac{GM}{4\pi r^4} dM$$

Using $p_{\text{surface}} = 0$,

$$p_{\text{centre}} > \frac{GM_T^2}{8\pi R^4} \quad (3.4)$$

and using equation (3.3),

$$4\pi r^3 dp = 3V dp = -\frac{GM}{r} dM$$

Here V denotes volume. Using Ω for total gravitational potential energy (a negative value),

$$3 \int_{p_{\text{centre}}}^{p_{\text{source}}} p dV + \Omega = 0$$

Using $dV = dM/\rho$, we obtain the Virial theorem for stars:

$$3 \int_0^{M_T} \frac{p}{\rho} dM + \Omega = 0 \quad (3.5)$$

However, this is incomplete as energy is also being produced in the nuclear fusion in the core, elongating the lifespan of star when calculated by energy methods.

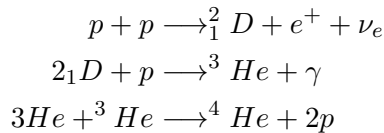
3.2.2 Equation of Energy Generation

The outflow of energy is given by:

$$dL = 4\pi r^2 \rho \epsilon dr \quad (3.6)$$

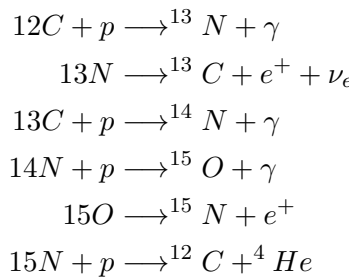
This energy comes from two types of fusion cycles:

- The p-p chain: This is the chain of nuclear fusion reaction in which protons get directly added to each other to form helium. This form of fusion is dominant below 1.7×10^7 K.



Here $\epsilon \propto \rho T^4$.

- The CNO cycle: This is the fusion cycle where C acts as a catalyst. It is dominant above 1.7×10^7 K. Here $\epsilon \propto \rho T^{17}$



3.2.3 Equation of Radiative Transport

Heat diffusion equation:

$$F = -\lambda dT/dr$$

Here λ is the heat diffusion coefficient and F is the power per unit area parallel to direction of temperature gradient. It is important to note that although radiation is scattered many times, its effect of transporting energy is still more important than conduction as movement of electrons is much slower.

$$dF = -K\rho F dr$$

Here K is opacity. The equation above describes how flux density decrease corresponds to decrease in radiation pressure. Thus the change in radiation pressure is given by:

$$dp = -\frac{K\rho F}{c} dr$$

. This gives us our fourth and final equation, listed in order of discussion:

$$\begin{aligned} \frac{dp}{dr} &= -\frac{GM\rho}{r^2} \\ \frac{dM}{dr} &= 4\pi r^2 \rho \\ \frac{dL}{dr} &= 4\pi r^2 \rho \epsilon \\ \frac{dT}{dr} &= -\frac{3K\rho}{16\pi a c r^2 T^3} \end{aligned} \tag{3.7}$$

3.3 Stellar Structure

Solving these equations we get some qualitative and quantitative results which are useful to keep in mind.

- In 1942 Chandrasekhar and Schonberg discovered that stars with an inert core with $> 10\%$ of the stellar mass cannot exist in stable equilibrium. The 10% figure actually signifies the ratio $(\frac{\mu_{core}}{\mu_{envelope}})^2$, where μ is the average molecular weight per electron and considers a plasma of hydrogen and helium in this case.
- We can come up with an approximate formula for calculating the main sequence lifespan of a star which burns H to He by the following relations:
 - Each Helium nucleus in the core was formed by emitting 0.7% of its total mass.
 - Thus total energy liberated by 10% of solar mass = $(0.007)M_{core}c^2$
 - Thus main sequence lifespan of the Sun

$$\begin{aligned} &= \frac{0.007 \times 0.1 \times M_T c^2}{L_o} \\ &\approx 10^{10} \text{ years} \end{aligned}$$

- In general,

$$T(M) = 10^{10} \left(\frac{M}{M_o}\right)^{-(x-1)}$$

Where $L \propto M^x$ for the given star

- We can come up with a simplified model of the Sun: a resonant sphere which when perturbed vibrates at frequencies corresponding to its normal modes of oscillations. These vibrations take place in the convective zone (where energy transfer takes place dominantly by convection), which is the outer 30% of its radius. The inner 70% is dominantly a radiative zone. The convective zone is responsible for most solar activity like solar flares and coronal mass ejections

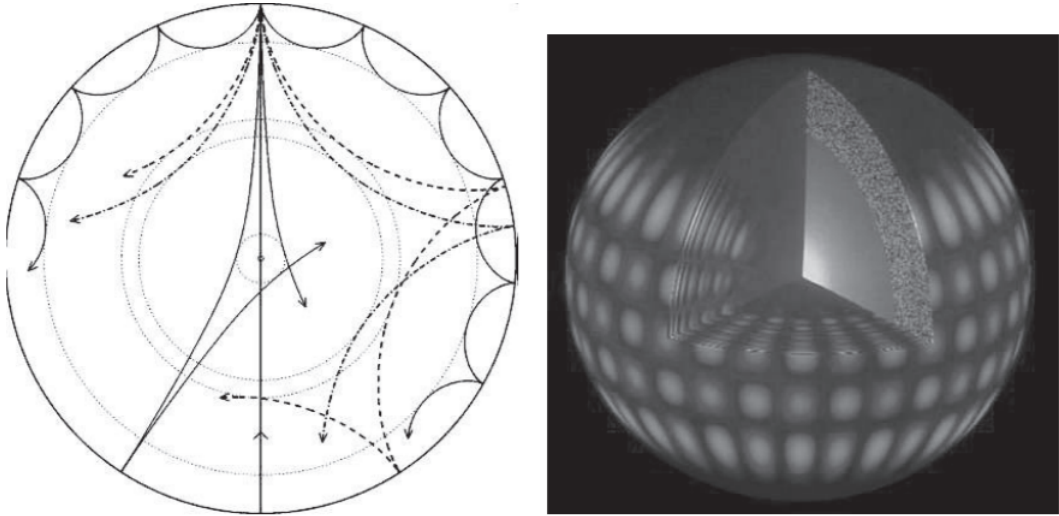


Figure 3.2: The figure on the left shows propagation of sound waves through a cross section of the sun (modelled). The figure on the right shows one of the natural modes of oscillations of the sun.[1]

3.4 Stellar Evolution

3.4.1 Hayashi Track

Hayashi in 1961 worked out the parameters for convective dominance vs radiative dominance. A region in a star is dominated by convective energy transfer if the temperature gradient exceeds the adiabatic gradient. The term ‘gradient’ here indicates derivative of temperature with respect to pressure. This is important to study as it affects the pre main sequence evolution, internal structure of stars and the red giant phase.

In general, radiative equilibrium dominates in stars lighter than the sun while convective equilibrium dominates in heavier stars. The sun in particular has regions of both convective and radiative dominance, as mentioned in the previous subsection. Since it is not completely related to High Energy Astrophysics, only a short explanation of it’s consequences will be given. High mass stars being convective will be able to continually renew the hydrogen fuel in the hottest part of the core and burn it up quickly, giving them short lifespans. Lower mass stars on the other hand will have cores with increasing amounts of Helium till the 10% limit is reached. Thus their fuel depletes slowly as fusion occurs in shells which are far from the hottest parts of the core.

3.4.2 High Mass Stars

The fate of high mass stars depends strongly on their mass. Thus we shall see the effects of higher and higher masses.

In general, when $M > 1.7 M_o$, CNO cycle dominates. For stars with masses at the lower

end of this spectrum, the core keeps burning H in the convective region till an inert core is formed. Once this happens, it rapidly expands its envelope and burns the remaining hydrogen in a shell. As the core collapses further, it starts to heat up further and fuses He to C .

In yet more massive stars, this newly formed C is fused to heavier elements till it reaches Fe , at which point further fusion requires more energy than it liberates. However in this process, the mechanism changes after reaching Si . It goes as follows. Some of the Si breaks into 7 He nuclei upon action by γ rays and this bombards all the elements increasing their weights by He addition. This creates onion-shell like layers in the star, with iron in the core.

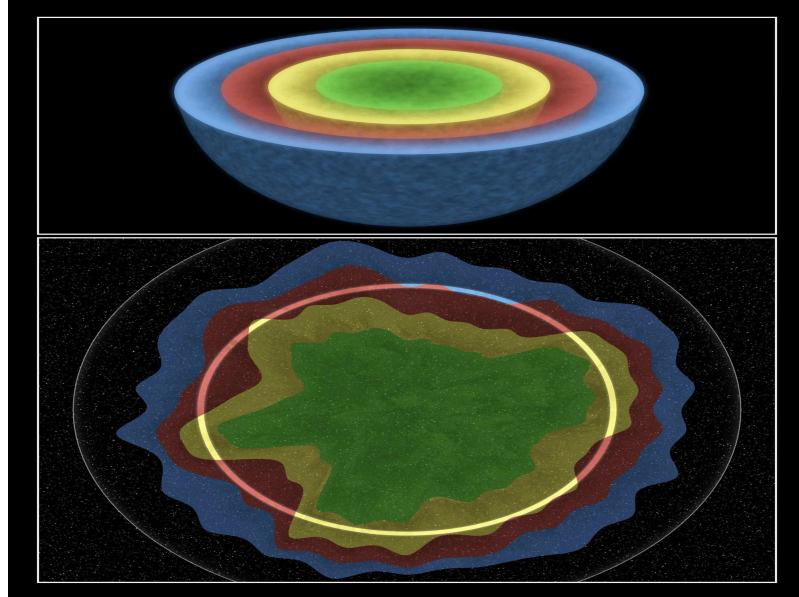


Figure 3.3: An artist's rendition of a star with onion-shell like structure and how it may be preserved in Cassiopeia A after blowing up in a supernova. [4]

Depending on how hot the core is, neutrons might get added to iron slowly (s-process) producing elements like Ba , Zr and Tc , or rapid process (r process) producing neutron rich species like heavy isotopes of tin - ^{122}Sn and ^{124}Sn .

3.4.3 Low Mass Stars

As we go lower and lower in mass range, the line between a star and exoplanet massive Jupiters begins to blur. Stars with mass lower than $0.08 M_o$ cannot fuse H in their core. Of these, $0.08 M_o > M > 0.01 M_o$ are brown dwarfs and $0.01 M_o > M > 0.001 M_o$ are exoplanets. Jupiter weighs $0.001 M_o$.

3.5 Mass Loss

3.5.1 P-Cygni Profiles and Wolf Rayet Stars

- P- Cygni Profiles: The stellar winds of stars absorb some of the light emitted, particularly the wavelength absorbed by line spectrum of the elements constituting the wind. In more extreme cases mass loss upto $10^{-4} M_o \text{ year}^{-1}$ is common. Stars with mass greater than $60 M_o$ lose mass at large rates as they cross the Eddington Limit (Section 6.2.5) - maximum mass where radiation pressure can balance gravity.

- In less extreme cases stars evolve to the red giant region and suffer mass loss from their surfaces. These are called Wolf-Rayet stars and typically lose $3 \times 10^{-5} M_o$ per year. They emit mostly UV and can have luminosities of almost $1000 L_o$. They have generally exhausted their hydrogen and are fusing heavier elements to the end of their lives. These are short phases and generally end in type Ib (no H lines in spectrum) or Ic (no H or He lines) supernovae.

Horizontal Branch

Stars of mass $\approx 2 M_o$ consume all their hydrogen in the core and inert helium core becomes degenerate. As the core heats up it starts to fuse He to C but without expanding due to some degeneracy effects. This is called helium flash and the star heats so much that the energy is comparable to the entire galaxy in the few minutes. Most of the energy, however, is absorbed by the star itself. Near this stage, these stars occupy the horizontal branch of the CMD.

Chapter 4

Galaxies

4.1 The Hubble Sequence

The Hubble sequence is a tuning fork like diagram which shows the evolution of galaxies. The handle of the tuning fork denotes elliptical galaxies, which are generally older, while the two arms of the fork show spiral galaxies and spiral-barred galaxies. Spiral barred galaxies have a centre bar shaped structure of composite stars with less spiral arms.

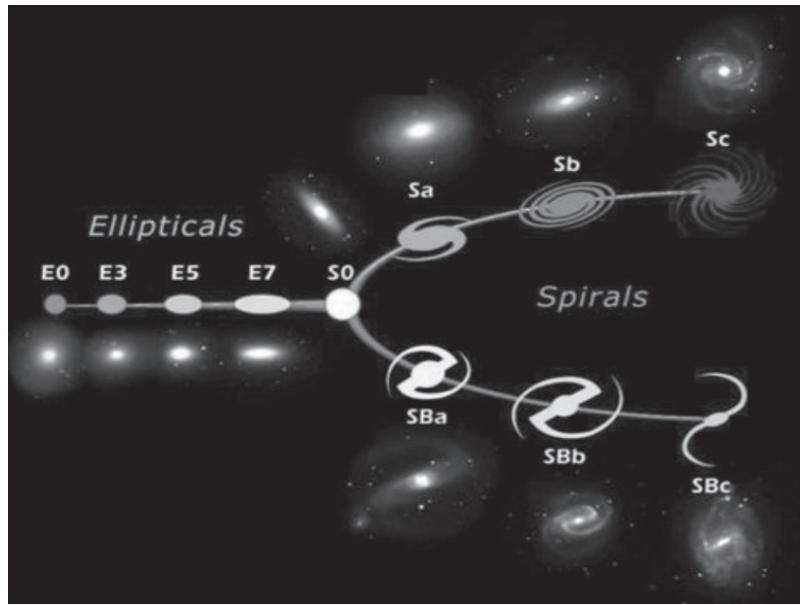


Figure 4.1: The Hubble sequence.[1]

Plotting these galaxies on a CMD, we get two major groups. These are the red sequence, which comprises of ‘old, red and dead’ galaxies and is spheroidal, while the other is blue cloud, which comprises of young, star forming and low mass galaxies which are disc dominated. They get their name from how they appear on the CMD.

4.2 Milky Way

- Sprial galaxies have a thin disc (95% of stars in it) and a thick disc with old stars having lower metal content.
- In particular, most of the Galaxy’s mass appears to lie more than 10 kpc from the center, where there are relatively few stars. We call this the dark matter and usually assume,

without a compelling reason, that it lies in a roughly spherical dark halo.

4.2.1 Gas in the Milky Way

- Fine structure transitions reflect the coupling between the electron's orbital angular momentum and its spin. Their wavelengths lie in the far infrared regions ($10 - 300 \mu\text{m}$ range for C , N and O)
- Hyperfine transitions are a consequence of coupling between the nuclear spin and the magnetic field generated by the orbiting electron. This results in the 21 cm line from H_I regions.

4.3 Other Galaxies

- To define a longitude on the sky, we use the vernal equinox as a zero point, like the Greenwich meridian on Earth. The 'longitude' of a star is its right ascension, denoted by α . Right ascension is measured eastward from the vernal equinox in hours, with 24 hours making up the complete circle.
- Surface Brightness of galaxies is not straightforward to think of as they don't appear as single points in the sky. Thus we define an equivalent formula to represent it:

$$I(\mathbf{x}) \equiv \frac{F}{\alpha^2} = \frac{L/(4\pi d^2)}{D^2/d^2} = \frac{L}{4\pi D^2}$$

Here the galaxy is approximately a square patch of side D , that we view from a distance d so that it extends an angle $\alpha = D/d$ on the sky. The combined luminosity of all stars is L and apparent brightness is F .

- It is not possible to observe the cores of far away galaxies in the infrared band directly from earth as the atmosphere is too bright even under ideal observing conditions.

4.3.1 Galaxies in the Expanding Universe

- In 1929, Edwin Hubble used some incredibly (numerically) inaccurate data of 22 galaxies and proposed that all galaxies in the universe are moving away from us at speeds given by the relation:

$$V_r \approx H_0 d$$

Subsequent work proved him right and this equation is now called Hubble's Law and H_0 is called Hubble's Constant. Its current value is debated to be between 60 and 75 $\text{km s}^{-1} \text{Mpc}^{-1}$. However this relation does not hold for galaxies in other clusters moving with some large 'peculiar' velocities within the cluster, changing the relation to

$$V_r = H_0 d + V_{pec}$$

- Scale length $\mathcal{R}(t)$ is a quantity which helps us know how the scale of the universe has changed with time. Hubble's Constant is given by $\dot{\mathcal{R}}(t_0)/\mathcal{R}(t_0)$. For the simplest models, $\mathcal{R}(t)$ depends only on the value of H_0 and the present density $\rho(t_0)$.
- The expansion of the universe plays a big role in affecting the light that we receive from far away galaxies. If the galaxies are close enough that $V_r \ll c$, we can rewrite the approximate formula for doppler shift to get

$$\frac{1}{\lambda} \frac{d\lambda}{dt} = \frac{1}{\mathcal{R}(t)} \frac{d\mathcal{R}(t)}{dt}$$

Integrating this gives us the cosmological redshift:

$$1 + z = \frac{\lambda_{obs}}{\lambda_e} = \frac{\mathcal{R}(t_0)}{\mathcal{R}(t_e)}$$

Here t_e is the time of emission. This relation holds for large redshifts as well as small.

4.4 Galaxy Clusters

- About half the galaxies in the Universe are found in groups and clusters, complexes where typically half the member galaxies are packed into a region $\lesssim 1$ Mpc across. Groups and clusters no longer expand with the cosmic flow: mutual gravitational attraction is strong enough that the galaxies are moving inward, or have already passed through the core. Clusters are the denser and richer structures, while groups are poorer associations.
- In contrast to groups, most baryonic matter in clusters is not actually part of the galaxies themselves but resides in intergalactic gas. In fact this dilute gas may account for 90% of the baryons in the universe. This gas is too cool to trace so we can only observe it through absorption effects.
- When two galaxies pass near each other, part of their energy of forward motion is transferred to motion of the stars within them. Thus they escape slower than they approached and if slowed down enough, they end up falling back towards each other and merging. This deceleration is described as dynamical friction. A high speed encounter drains less energy from their forward motion than a slow passage. However this is only true when we can ignore the random motion of the stars when compared to the forward motion of the galaxy.

After a galaxy collision though, when the galaxy has time to settle back, the combination of rotational motion and random speeds within each galaxy will be lower than before the collision. This is because the additional stellar speeds will expand the galaxy and is less strongly bound. Additionally, some stars escape or form a loose envelope around the galaxy.

If two galaxies pass each other in a typical rich galaxy cluster, they will most likely have enough energy to escape each other. However galaxies in typical groups have lower velocities and end up merging. Almost all galaxies we see undergoing mergers are parts of groups.

- A very close encounter or merger of two galaxies compresses their gas and causes a phase called starburst: stars form so rapidly so as to exhaust the gas supply within a few hundred million years. The encounter brings a lot of the gas towards the centre and gets squeezed by gravity resulting in violent star formation. After this dies away, it may leave a bright compact inner disk of stars.

Chapter 5

Important Physical Processes

5.1 Nuclear Interactions

5.1.1 Introduction

Nuclear physics is central to many branches of astrophysics, in particular to the understanding of the processes of energy generation in stars. In these cases, the nuclear processes occur deep in the centres of stars where the products of nucleosynthesis are generally only indirectly observable. The important exceptions to this statement are the observations of neutrinos from the Sun and the supernova SN 1987A.

Nuclear interactions are only important when the incident high energy particle makes a more or less direct hit on the nucleus because the strong forces which hold the nucleus together are short range. Thus, the cross-section for nuclear interactions, in the sense that some form of interaction with the nucleons takes place, is just the geometric cross-section of the nucleus. A suitable expression for the radius of the nucleus is

$$R = 1.2 \times 10^{-15} A^{1/3} \text{ m}$$

where A is the mass number. In many cases high energy particles have energies greater than 1 GeV. This introduces a further factor since at these energies the de Broglie wavelength of the incident particle is small compared to the distance between nucleons in a nucleus. For example the effective ‘size’ of an incident proton of energy 10 GeV can be estimated by Heisenberg’s relation as

$$\Delta x \approx \hbar/p = \hbar/\gamma m_p v = 0.02 \times 10^{-15} \text{ m}$$

Thus we can consider an incident proton to be a discrete, very small particle which can interact with the individual nucleons within the nucleus. The number of particles with which it interacts is just the number of nucleons along the line of sight through the nucleus. For example, a proton passing through an oxygen or nitrogen nucleus interacts, on average, with about $15^{1/3}$, that is, 2.5 of the nucleons. In fact the incident proton can be considered to be scattered multiple times within the nucleus.

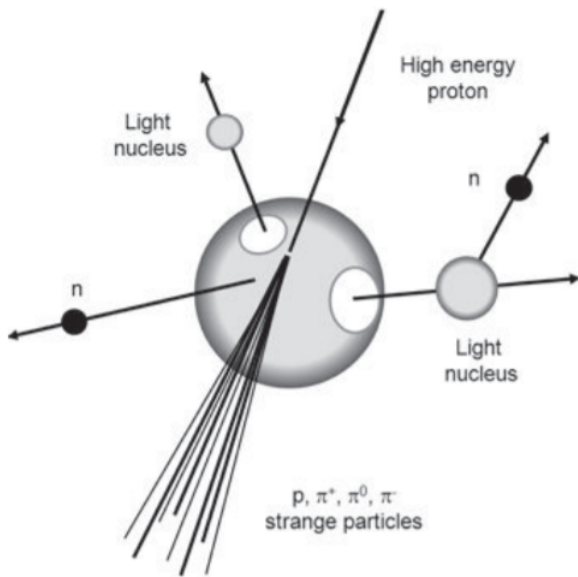


Figure 5.1: Principal products of a high energy proton colliding with a nucleus. [1]

The general picture can be described by the following rules.

- Protons interact strongly with an individual nucleon and produce a shower of pions of all charges, π , π^+ , π^- , and occasionally strange particles and even anti nucleons.
- In the centre of momentum reference frame of the encounter, the pions generally emerge in forward or backward directions but may have lateral momenta of the order of $\approx 100 - 200 \text{ MeV c}^{-1}$
- The nucleons and pions possess very high forward momenta through the laboratory frame of reference and are thus high energy particles.
- Secondary particles after the first collision may interact with further particles in the nucleus provided the first collision took sufficiently close to the front end of the nucleus. Thus a mini-nucleonic cascade is initiated.
- Only one or two nucleons participate in the nuclear interactions with the high energy particle and are generally removed from the nucleus in a high energy state. The resulting nucleus may not be in a stable state and as a result of this several nuclear fragments may be evaporated from it. These are called spallation fragments and are related to the origin of light nuclei as cosmic rays. These particles are emitted from the reference frame of the resultant nucleus which does not gain much momentum from the collision due to high energies required in overcoming the strong nuclear force. Thus these particles come out isotropically in the laboratory frame of reference.

For protons of incident energies $> 1 \text{ GeV}$ a useful empirical rule is that for each collision roughly $2E^{1/4}$ high energy charged particles are produced (where E is measured in GeV, though they might not always be pions).

5.1.2 Spallation cross-sections

The details of cross sections for production many spallation products is an important topic of study as it highly affects the propagation of cosmic ray nuclei in interstellar medium. There are many approaches to try to determine this observationally or semi empirically.

One important method of doing this by simulating the details of particle-particle collisions using

the Monte Carlo method. The trajectory of the incoming particle is followed after selecting the initial conditions randomly. Depending upon the particles which are knocked off the nucleus. The probability of different end products being formed helps find their partial cross sections. Typically this is carried out on high speed computers so that good statistics can be built up for even rare interactions.

Observational data from the cases that we can create in labs provides some interesting and useful insights. Firstly there is always a large cross section for chipping off a single nucleon or alpha particle. This is understandable as most collisions are grazing ones and not head on. When product nuclei are unstable, formation of pairs of nuclei of similar masses is not favoured, as similarly seen in fission. Secondly it was found that even nuclei are favoured slightly over odd nuclei. This parallels the observed abundances of elements which favour even nuclei when we see them as a whole.

The cross sections also depend on energy. Plotting the graph for observed data and theoretical data gives an insight into the validity of our theories. For formation of smaller elements from C^{12} and O^{16} , the variation in observed and predicted partial cross sections are quite small. However, for iron nuclei there are strong variations in the partial spallation cross sections at low energies. These variations are principally associated with the difference in mass number of the parent and product nuclei. At relativistic energies, it is expected that the cross-sections should remain roughly constant and the semi-empirical formulae provided an accurate description of the partial cross-sections.

5.1.3 Nuclear Emission Lines

There are two important nuclear processes which produce γ -ray lines: the decay of radioactive species and the collisional excitation of the nuclei by cosmic ray protons.

Decay of Radioactive Isotopes

Stellar nucleosynthesis produces nuclei which may or may not be stable, the latter being sources of γ -rays. For these to be observable there must be large enough yields of these unstable nuclei and their half lives should be sufficiently short.

In order to be observable the radioactive nuclei must be ejected from the source so that the γ -rays do not get absorbed within the interior of the star. This has to be the case for radionucleides with half lives less than one year. For longer lived species, the nuclei can be brought to the surface via convection such as in cases like Wolf-Rayet stars. Thus it is expected that emissions related to shorter half lives are expected to come from point like sources such as supernovae, while the rest are observed from directions throughout the galactic plane. Because of this predictable distribution, it is possible to determine the average supernova rate for the galaxy as a whole.

Collisional Excitation of Nuclei

Nuclei are excited by collisions with cosmic ray protons and they subsequently get deexcited by emission of γ -rays. These interactions may take place in either the diffuse interstellar gas, in which case the target nuclei attain high velocities, or in interstellar grains (dust like particles made of carbon, silicon, oxygen or other elements) in which case the γ -rays are emitted essentially at rest.

5.2 Ionisation Losses

When high energy particles pass through solids, liquids or gases, they cause considerable wreckage. Particularly,

- The ionisation and excitation of atoms and molecules in the material. This not only ionises the material by the electromagnetic attraction by the particle, but also causes heating by transfer of kinetic energy.
- Destruction of crystal structures and molecular chains.
- Nuclear interactions between the cosmic ray particle and the material.

Ionisation losses are an important topic of study to understand the propagation of high energy cosmic rays through the interstellar medium and the heating of interstellar gas. Studying this also helps particle detectors to consider all phenomena.

5.2.1 Non Relativistic Treatment

Consider an interaction between a high energy particle and a stationary electron. Only a very small fraction of the high energy particle's kinetic energy is transferred to the electron as is expected due to the low mass of electron. The maximum velocity from this interaction can be $2v$, where v was the velocity of the incident particle. Thus the maximum fractional loss in kinetic energy can be $4m_e/M$ where M is the mass of incident particle and m_e the mass of electron.

Using this first qualitative result we can make the assumption that the incident particle remains essentially undeviated and the electron remains stationary. The charge of high energy particle is ze , the mass is M , the distance of closest approach, called the collision parameter, is b . The total momentum imparted to the particle is $\int F dt$. By symmetry, the forces parallel to the line of flight cancel out and thus we need to consider only work done in perpendicular component.

$$F_{\perp} = \frac{ze^2}{4\pi\epsilon_0 r^2} \sin\theta; \quad dt = \frac{dx}{v}$$

Using $b/x = \tan\theta$, $r = b/\sin\theta$ and therefore $dx = (-b/\sin^2\theta) d\theta$, v is essentially constant and thus momentum impulse is

$$\int_{\infty}^{\infty} F_{\perp} dt = - \int_0^{\pi} \frac{ze^2}{4\pi\epsilon_0 b^2} \sin^2\theta \frac{b \sin\theta}{v \sin^2\theta} d\theta = - \frac{ze^2}{4\pi\epsilon_0 bv} \int_0^{\pi} \sin\theta d\theta$$

Therefore the momentum impulse is

$$p = \frac{ze^2}{2\pi\epsilon_0 bv}.$$

Thus kinetic energy transferred is

$$\frac{p^2}{2m_e} = \frac{z^2 e^4}{8\pi^2 \epsilon_0^2 b^2 v^2 m_e}$$

Which is the energy loss by high energy particle.

We now need to find the average loss per unit length and so work out the number of collision parameters in the range b to $b+db$ and integrate over collision parameters. From geometry, the total energy loss $-dE$ in length dx is

$$\begin{aligned} & (\text{number of electrons in volume } 2\pi b db dx) \times (\text{energy loss per interaction}) \\ &= \frac{z^2 e^4 N_e}{8\pi^2 \epsilon_0^2 v^2 m_e} \int_{b_{min}}^{b_{max}} \frac{2\pi b}{b^2} db dx \end{aligned}$$

where N_e is the number density of electrons. On integrating we obtain

$$-\frac{dE}{dx} = \frac{z^2 e^4 N_e}{4\pi\epsilon_0^2 v^2 m_e} \ln \frac{b_{max}}{b_{min}} \quad (5.1)$$

This non relativistic treatment gives a remarkably accurate result as b_{max} and b_{min} do not need to be very accurate as they are inside the logarithm. Now the important thing is to determine the possible values of b_{max} and b_{min} .

Upper Limit b_{max} :

An upper limit to collision parameter, corresponding to the smallest energy transfer, occurs when duration of collision is of the same order as the period of the electron. The interaction is no longer impulsive. In the limit where the duration of collision is much greater than the period of electron, it feels a slowly varying weak field and thus avoids ionisation by ‘conserving motion adiabatically’.

The duration of the collision can be understood through the following derivation. If we take the time during which the particle feels a strong interaction with the electron to be $\tau = 2b/v$ and multiply by the electrostatic force at the distance of closest approach,

$$F = ze^2/4\pi\epsilon_0 b^2; \text{ momentum impulse } p = F\tau = \frac{ze^2}{2\pi\epsilon_0 bv}$$

If the collision time is of the same order as the orbital period of the electron, we obtain an order of magnitude for b_{max} . Hence,

$$2b_{max}/v \approx 1/\nu_0$$

where ν_0 is the orbital frequency of the electron. Writing $\omega_0 = 2\pi\nu_0$,

$$b_{max} \approx \frac{v}{2\nu_0} = \frac{\pi v}{\omega_0}$$

Lower Limit b_{min}

There are two possibilities for having a b_{min} . These are:

- According to classical physics the distance of closest approach is minimum when the electrostatic energy of the particle and electron is equal to the maximum energy transfer possible. This value is $2m_e v^2$. Thus

$$ze^2/4\pi\epsilon_0 b_{min} \approx 2m_e v^2; \quad b_{min} = ze^2/8\pi\epsilon_0 m_e v^2$$

However if this amount of energy is transferred during the interaction, the electron would move by a distance of order of b_{min} during the encounter and thus the assumption giving us an accurate answer breaks down.

- A second possible value is obtained when we perform a quantum mechanical calculation to describe close encounters. The max velocity of electron in this encounter is $\Delta v = 2v$ and hence change in momentum is $\Delta p = 2m_e v$. There is therefore a corresponding uncertainty in position giving us $b_{min} = \hbar/2m_e v$. Granted this defect in our calculation, this should still give us the least possible meaningful value for the integral limit b_{min} .

We choose the larger value of b_{min} for the calculation for the physical conditions of the problem. The ratio of possible values of b_{min} is:

$$\frac{b_{min}(\text{quantum})}{b_{min}(\text{classical})} = \frac{\hbar}{2m_e v} \frac{8\pi\epsilon_0 m_e v^2}{ze^2} = \frac{4\pi\epsilon_0 v\hbar}{ze^2} = \frac{1}{z\alpha} \left(\frac{v}{c}\right) = \frac{137}{z} \left(\frac{v}{c}\right) \quad (5.2)$$

where $\alpha = e^2/4\pi\epsilon_0 c\hbar \approx 1/137$ is the fine structure constant. Thus if v/c is greater than 0.01, the quantum limit should be used.

5.2.2 The Relativistic Case

The logic to calculate the relativistic case is pretty similar and thus we need to calculate the electrostatic inverse square law for source of electric field in the relativistic case. This is an important calculation and will reappear many times throughout the course of this topic.

We orient the reference frames S and S' in standard configuration with the high energy particle moving along the positive x-axis and the electron located at a distance b along the z-axis in S. The coordinate systems are set up so that $t = t' = 0$ and $x = x' = 0$ when the high energy particle is at its distance of closest approach in S. At time t, the particle is located at x in S. In S', the coordinates of the electron (or its displacement four-vector) are $[ct', vt', 0, b]$ (A point at a given time, called an event or four vector, is given by $4[ct, \mathbf{r}]$ where \mathbf{r} is the position vector in 3 dimensional space). Furthermore, in S' the electric field E of the particle is spherically symmetric about the origin 0' and hence, at the electron,

$$E_{x'} = \frac{ze}{4\pi\epsilon_0 r^2} \cos\theta' = -\frac{ze}{4\pi\epsilon_0 r'^3},$$

$$E_{z'} = \frac{ze}{4\pi\epsilon_0 r^2} \sin\theta' = -\frac{ze}{4\pi\epsilon_0 r'^3},$$

where $r'^2 = (vt')^2 + b^2$ and θ' is the angle between positive x axis and direction of electron in S'. We now relate the time measured by the stationary observer on the electron in S to that measured by the observer moving with high energy particle,

$$ct' = \gamma \left(ct - \frac{vx}{c} \right)$$

But by our choice of coordinates, $x = 0$ for the electron in S and hence $t' = \gamma t$. Therefore,

$$E_{x'} = -\frac{ze(\gamma vt)}{4\pi\epsilon_0 [b^2 + (\gamma vt)^2]^{1/2}},$$

$$E_{z'} = -\frac{zeb}{4\pi\epsilon_0 [b^2 + (\gamma vt)^2]^{1/2}},$$

Using the inverse lorentz transformations to find E and B ,

$$E_x = E_{x'}; \quad B_x = B_{x'}$$

$$E_y = \gamma(E_{y'} + vB_{z'}); \quad B_y = \gamma(B_{y'} - \frac{v}{c^2}E_{z'})$$

$$E_z = \gamma(E_{z'} + vB_{y'}); \quad B_y = \gamma(B_{z'} + \frac{v}{c^2}E_{y'})$$

Since $B_{x'} = B_{y'} = B_{z'} = 0$ in S', we find

$$E_x = -\frac{\gamma zevt}{4\pi\epsilon_0 [b^2 + (\gamma vt)^2]^{3/2}} \quad B_x = 0 \quad (5.3)$$

$$E_y = 0 \quad B_y = -\frac{\gamma zevb}{4\pi\epsilon_0 c^2 [b^2 + (\gamma vt)^2]^{3/2}} \quad (5.4)$$

$$E_z = -\frac{\gamma zeb}{4\pi\epsilon_0 [b^2 + (\gamma vt)^2]^{3/2}} \quad B_z = 0 \quad (5.5)$$

$$(5.6)$$

Relativistic Ionisation Losses

Because of the symmetry of E_x about $t = 0$, there is no net momentum imparted on electron in x direction. However there is net momentum in z direction,

$$F_z dt = \frac{ze^2\gamma b}{4\pi\epsilon_0} \int_{\infty}^{\infty} \frac{dt}{[b^2 + (\gamma vt)^2]^{3/2}}$$

Solving the integral by substitution we get

$$\text{Momentum Impulse} = \frac{ze^2}{2\pi\epsilon_0 vb} \quad (5.7)$$

which is exactly the same as the non relativistic case. This was expected as the argument in the non relativistic section indicated that it is the product of E_z and the collision parameter and while E_z increases by a factor of γ , τ decreases by the same factor.

The integration over collision parameters proceeds as in the non relativistic case so all we need to worry about are the values of b_{max} and b_{min} . In the first approach, b_{max} is greater by a factor of γ because the duration of impulse is shorter by this factor. In the case of b_{min} , the transverse momentum of electron is greater by a factor of γ and hence because of the Heisenberg's uncertainty principle, b_{min} is lower by a factor of γ . Thus we expect the term in the logarithm to be increased by a factor of γ^2 .

5.2.3 Ionisation Losses of Electrons

There are two important differences between the ionisation losses of electrons and protons or nuclei. The first being the interacting particles, high energy electrons and thermal electrons, are identical. The second is that electrons suffer much larger deviations in the electrons. The net result is not so different from before though. The formula of ionisation losses for an electron with energy $\gamma m_e c^2$ is

$$-\frac{dE}{dx} = \frac{e^4 N_e}{8\pi\epsilon_0^2 m_e v^2} \left[\ln \frac{\gamma m_e v^2 E_{max}}{2\bar{I}^2} - \left(\frac{2}{\gamma} - \frac{1}{\gamma^2} \right) \ln 2 + \frac{1}{\gamma^2} + \frac{1}{8} \left(1 - \frac{1}{\gamma} \right)^2 \right]$$

Where N_e is the number density of ambient electrons, E_{max} is the maximum kinetic energy which can be transferred to an electron in a single interaction and \bar{I} is the weighted average of ionisation energy of atoms with electrons in all possible states. Similar to a proton or nucleus colliding with an electron, we calculate the maximum kinetic energy transfer to be

$$E_{max} = \frac{2\gamma^2 M^2 m_e v^2}{m_e^2 + M^2 + 2\gamma m_e M}$$

where M is the rest mass of fast moving particle, v its velocity and γ its corresponding Lorentz factor. Differences are found when loss rates are compared for protons and electrons of same kinetic energy. The loss rate of protons is higher than that of electrons until the particles become relativistic. The physical reason for this is proton of same kinetic energy as an electron moves slower and hence there is a larger momentum imparted onto the electrons. However at relativistic speeds this difference in interaction time becomes less significant.

5.3 Radiation of Accelerated Charged Particles

Bremsstrahlung, or free-free emission, appears in many different guises in astrophysics. Applications include the radio emission of compact regions of ionised hydrogen at temperature $T \approx 10^4$ K, the X-ray emission of binary X-ray sources at $T \approx 10^7$ K and the diffuse X-ray emission of intergalactic gas in clusters of galaxies, which may be as hot as $T \approx 10^8$ K. It is also an important loss mechanism for relativistic cosmic ray electrons.

5.3.1 Relativistic Invariants

Before the details of the phenomena related to radiation are covered, it is helpful to know some relativistic invariants in electromagnetic processes. The first is the energy loss rate by electromagnetic radiation as observed in different inertial frames of reference. dE/dt is a Lorentz invariant between inertial frames of reference. This can be shown by the following argument. In the moving instantaneous rest frame of an accelerated charged particle, the total energy loss dE' has dipole symmetry and so is emitted with net zero momentum. Thus its four-momentum can be written $[dE'/c, 0]$. This radiation is emitted in interval of dt' which is the zeroth component of the displacement four-vector $[c dt', 0]$. Using inverse Lorentz transforms to relate dE' and $c dt'$ to dE and $c dt$, we find

$$dE = \gamma dE'; \quad dt = \gamma dt'$$

and hence

$$dE/dt = dE'/dt' \quad (5.8)$$

5.3.2 The Radiation of Accelerated Charged Particle

The standard analysis begins with Maxwell's equations in free space:

$$\nabla \times \mathbf{E} = -\frac{\partial \mathbf{B}}{\partial t} \quad (5.9)$$

$$\nabla \times \mathbf{B} = \mu_0 \mathbf{J} + \frac{1}{c^2} \frac{\partial \mathbf{E}}{\partial t} \quad (5.10)$$

$$\nabla \cdot \mathbf{B} = 0 \quad (5.11)$$

$$\nabla \cdot \mathbf{E} = \rho_e/\epsilon_0 \quad (5.12)$$

To help analyse and simplify the calculation it is helpful to introduce scalar and vector potentials, ϕ and \mathbf{A} respectively. These are defined as

$$\mathbf{B} = \nabla \times \mathbf{A} \quad (5.13)$$

$$\mathbf{E} = -\frac{\partial \mathbf{A}}{\partial t} - \nabla \phi \quad (5.14)$$

The reason for this is that the fields \mathbf{E} and \mathbf{B} are the components of a four-tensor. It is thus much easier to work in terms of the four-vector potential $[\phi/c, \mathbf{A}]$ and then take the derivatives (5.13) to find \mathbf{E} and \mathbf{B} . Substituting in the second Maxwell's equation,

$$\nabla \times (\nabla \times \mathbf{A}) = \mu_0 \mathbf{J} - \frac{1}{c^2} \frac{\partial}{\partial t} \left(\frac{\partial \mathbf{A}}{\partial t} + \nabla \phi \right) \quad (5.15)$$

Thus expanding and interchanging order of time and spacial derivatives:

$$\nabla^2 \mathbf{A} - \frac{1}{c^2} \frac{\partial^2 \mathbf{A}}{\partial t^2} = -\mu_0 \mathbf{J} + \nabla \left[\nabla \cdot \mathbf{A} + \frac{1}{c^2} \frac{\partial \phi}{\partial t} \right] \quad (5.16)$$

Making the same substitutions for \mathbf{E} and \mathbf{B} in the fourth Maxwell's equation and interchanging the order of differentiation,

$$\frac{\partial}{\partial t} (\nabla \cdot \mathbf{A}) + \nabla^2 \phi = -\frac{\rho_e}{\epsilon_0} \quad (5.17)$$

Now add $(1/c^2)(\partial^2 \phi / \partial t^2)$ to both sides,

$$\nabla^2 \phi - \frac{1}{c^2} \frac{\partial^2 \phi}{\partial t^2} = -\frac{\rho_e}{\epsilon_0} - \frac{\partial}{\partial t} \left[\nabla \cdot \mathbf{A} + \frac{1}{c^2} \frac{\partial \phi}{\partial t} \right] \quad (5.18)$$

The equations (5.16) and (5.18) have remarkably similar forms and we would obtain two simple inhomogeneous wave equations for \mathbf{A} and ρ separately if we were able to set the quantities in the square brackets equal to zero. Fortunately, we can do that as \mathbf{A} only appears as the quantity which when curled results in the magnetic field \mathbf{B} which is what we measure in the laboratory. We can always add the gradient of a scalar quantity to \mathbf{A} and it will always disappear on curling. On writing $\mathbf{A}' = \mathbf{A} + \text{grad } \chi$, substituting in (5.13) gives the substitution $\phi' = \phi - chi$. Using this and simplifying, we can find a suitable function by the method of Lorentz gauge to give the pair of equations:

$$\nabla^2 \mathbf{A} - \frac{1}{c^2} \frac{\partial^2 \mathbf{A}}{\partial t^2} = -\mu_0 \mathbf{J} \quad (5.19)$$

$$\nabla^2 \phi - \frac{1}{c^2} \frac{\partial^2 \phi}{\partial t^2} = -\frac{\rho_e}{\epsilon_0} \quad (5.20)$$

These equations have standard forms of solution:

$$\mathbf{A}(\mathbf{r}) = \frac{\mu_0}{4\pi} \int \frac{\mathbf{J}(\mathbf{r}', t - |\mathbf{r} - \mathbf{r}'|/c)}{|\mathbf{r} - \mathbf{r}'|} d^3 \mathbf{r}' \quad (5.21)$$

$$\phi(\mathbf{r}) = \frac{1}{4\pi\epsilon_0} \int \frac{\rho_e(\mathbf{r}', t - |\mathbf{r} - \mathbf{r}'|/c)}{|\mathbf{r} - \mathbf{r}'|} d^3 \mathbf{r}' \quad (5.22)$$

The Non Relativistic Case:

The fields are measured at \mathbf{r} and the integration is over electric current and charge distributions throughout space. The terms $|\mathbf{r} - \mathbf{r}'|/c$ take account of the fact that current and charge distributions should be evaluated at retarded times. Firstly, for an accelerated charged particle, the integral of the product of the current density \mathbf{J} and the volume element $d^3 \mathbf{r}'$ is just the product of its charge times its velocity,

$$\int \mathbf{J} \left(\mathbf{r}', t - \frac{|\mathbf{r} - \mathbf{r}'|}{c} \right) d^3 \mathbf{r}' = q\mathbf{v}\delta(\mathbf{r})$$

where $\delta(\mathbf{r})$ is the Dirac delta function. The expression for vector potential is therefore

$$\mathbf{A} = \frac{\mu_0 q \mathbf{v}}{4\pi r} \quad (5.23)$$

Taking the time derivative of \mathbf{A} in order to find \mathbf{E} ,

$$\mathbf{E} = -\frac{\partial \mathbf{A}}{\partial t} = -\frac{\mu_0 q \ddot{\mathbf{r}}}{4\pi r} = -\frac{q \ddot{\mathbf{r}}}{4\pi\epsilon_0 c^2 r}$$

Writing this in angular form and using $q\mathbf{a} = \ddot{\mathbf{p}}$, where \mathbf{p} is the electric dipole moment of charge with respect to some origin,

$$E_\theta = \frac{|\ddot{\mathbf{p}}| \sin \theta}{4\pi\epsilon_0 c^r}$$

This electric field component represents a pulse of electromagnetic radiation, and hence the rate of energy flow per unit area per second at distance r is given by the magnitude of the Poynting vector $S = |\mathbf{E} \times \mathbf{H}| = E^2/Z_0$ where $Z_0 = (\mu_0/\epsilon_0)$ is the impedance of free space. The rate of energy flow through the area $r^2 d\Omega$ subtended by solid angle $d\Omega$ at angle θ and at distance r from the charge is therefore

$$Sr^2 d\Omega = -\left(\frac{dE}{dt}\right) d\Omega = \frac{|\ddot{\mathbf{p}}|^2 \sin^2 \theta}{16\pi^2 Z_0 \epsilon_0^2 c^6 4r^2} r^2 d\Omega = \frac{|\ddot{\mathbf{p}}|^2 \sin^2 \theta}{16\pi^2 \epsilon_0^2 c^3} d\Omega \quad (5.24)$$

To find the total radiation rate, we integrate over the solid angle. Because of the symmetry of the emitted intensity with respect to the acceleration vector, we can integrate over the solid angle defined by the circular strip between the angles θ and $\theta + d\theta$, $d\Omega = 2\pi \sin \theta d\theta$:

$$-\left(\frac{dE}{dt}\right) = \int_0^\pi \frac{|\ddot{\mathbf{p}}|^2 \sin^2 \theta}{16\epsilon_0 c^3} 2\pi \sin \theta d\theta \quad (5.25)$$

We find the result

$$-\left(\frac{dE}{dt}\right) = \frac{|\ddot{\mathbf{p}}|^2}{6\pi\epsilon_0 c^3} = \frac{q^2 |\mathbf{a}|^2}{6\pi\epsilon_0 c^3} \quad (5.26)$$

This result is sometimes referred to as Larmor's formula. These formulae embed three important properties of the radiation of an accelerated charged particle:

- The total radiation rate is given by Larmor's formula. In this formula, the acceleration is the proper acceleration of the charged particle in the relativistic sense and that the radiation loss rate is that measured in the instantaneous rest frame of the particle, such as a body in free fall or an inertial frame.
- The electric field strength varies as $\sin \theta$ and the power radiated per unit solid angle varies as $\sin^2 \theta$ where θ is the angle with respect to the acceleration vector of the particle. There is no radiation along the acceleration vector and the field strength is greatest at right angles to it.
- The radiation is polarised, the electric field vector, as measured by a distant observer, lying in the direction of the acceleration vector of the particle as projected onto the sphere at distance \mathbf{r} from the charged particle.

Another important point to note is that these results are correct provided the velocities of the charges are small. A more complete analysis (beyond the scope of this report) leads to Lienard-Wiechert potentials which are valid at all velocities:

$$\mathbf{A}(\mathbf{r}, t) = \frac{\mu_0}{4\pi r} \left[\frac{q\mathbf{v}}{1 - (\mathbf{v} \cdot \mathbf{n})/c} \right]_{ret} ; \quad \phi(\mathbf{r}, t) = \frac{1}{4\pi\epsilon_0 r} \left[\frac{q}{1 - (\mathbf{v} \cdot \mathbf{n})/c} \right]_{ret} \quad (5.27)$$

where \mathbf{n} is the unit vector in the direction of the point of observation from the moving charge. In both the cases, the potentials are evaluated at retarded times relative to the location of the observer. It is important to look into these potentials as the terms in the denominators of (5.27) will reappear in a number of occasions. For example, the case when the particle moves towards the point of observation at a velocity close to that of light, it represents the fact that the particle almost catches up with the radiation it emits.

The Relativistic Case

It is assumed that, in the particle's instantaneous rest frame, the acceleration of the particle is small and this is normally the case. The following general results are needed: first, the norm of the acceleration four-vector is an invariant in any inertial frame of reference and, second, the acceleration four-vector of the particle, \mathbf{A} , not to be confused with the vector potential \mathbf{A} of the last section, can be written

$$\mathbf{A} = \gamma \left[c \frac{\partial \gamma}{\partial t}, \frac{\partial(\gamma \mathbf{v})}{\partial t} \right] = \left[\left(\frac{\mathbf{v} \cdot \mathbf{a}}{c^2} \right) \gamma^4 c, \gamma^2 \mathbf{a} + \left(\frac{\mathbf{v} \cdot \mathbf{a}}{c^2} \right) \gamma^4 \mathbf{v} \right] \quad (5.28)$$

where the acceleration $\mathbf{a} = \ddot{\mathbf{r}}$ and the velocity of the particle $\mathbf{v} = \dot{\mathbf{r}}$ are measured in the observer's frame of reference S. In the instantaneous rest frame of the particle, S', the acceleration four

vector is $[0, \mathbf{a}_0]$ where $\mathbf{a} = (\ddot{\mathbf{r}})_0$ is the proper acceleration of the particle. Equating the norms of the four vectors in both the frames and simplifying:

$$\mathbf{a}_0^2 = \gamma^4 [\mathbf{a}^2 + \gamma^2 (\mathbf{v} \cdot \mathbf{a}/c^2)]$$

Since the radiation rate (dE/dt) is Lorentz invariant,

$$\left(\frac{dE}{dt} \right)_S = \left(\frac{dE'}{dt'} \right)_{S'} = \frac{q^2 |\mathbf{a}_0|^2}{6\pi\epsilon_0 c^3} = \frac{q^2 \gamma^4}{6\pi\epsilon_0 c^3} \left[\mathbf{a}^2 + \gamma^2 \left(\frac{\mathbf{v} \cdot \mathbf{a}}{c} \right)^2 \right] \quad (5.29)$$

$$\left(\frac{dE'}{dt'} \right)_{S'} = \frac{q^2 \gamma^4}{6\pi\epsilon_0 c^3} (|a_\perp|^2 + \gamma^2 |a_\parallel|^2) \quad (5.30)$$

Parseval's Theorem and the Spectral Distribution of Radiation

Using the Parseval's theorem we can find an elegant solution to the distribution of radiation field of the electron into its spectral components. To begin we overview the Fourier transform pair for the acceleration of the particle:

$$\dot{\mathbf{v}}(t) = \frac{1}{(2\pi)^{1/2}} \int_{-\infty}^{\infty} \dot{\mathbf{v}}(\omega) \exp(-i\omega t) d\omega \quad (5.31)$$

$$\dot{\mathbf{v}}(\omega) = \frac{1}{(2\pi)^{1/2}} \int_{-\infty}^{\infty} \dot{\mathbf{v}}(t) \exp(i\omega t) dt \quad (5.32)$$

According to Parseval's theorem, $\dot{\mathbf{v}}(t)$ and $\dot{\mathbf{v}}(\omega)$ are related by the following integral:

$$\int_{-\infty}^{\infty} |\dot{\mathbf{v}}(\omega)|^2 d\omega = \int_{-\infty}^{\infty} |\dot{\mathbf{v}}(t)|^2 dt \quad (5.33)$$

This is proved in most textbooks on Fourier analysis. Applying this relation to energy radiated by a particle with an acceleration history $\dot{\mathbf{v}}(t)$:

$$\int_{-\infty}^{\infty} \frac{dE}{dt} dt = \int_{-\infty}^{\infty} \frac{e^2}{6\pi\epsilon_0 c^3} |\dot{\mathbf{v}}(t)|^2 dt = \int_{-\infty}^{\infty} \frac{e^2}{6\pi\epsilon_0 c^3} |\dot{\mathbf{v}}(\omega)|^2 d\omega$$

Since acceleration is a real function, we can use

$$\int_{-\infty}^0 |\dot{\mathbf{v}}(\omega)|^2 d\omega = \int_0^{\infty} |\dot{\mathbf{v}}(\omega)|^2 d\omega$$

and hence we find

$$\text{Total emitted radiation} = \int_0^{\infty} I(\omega) d\omega = \int_0^{\infty} \frac{e^2}{3\pi\epsilon_0 c^3} |\dot{\mathbf{v}}(\omega)|^2 d\omega$$

Therefore

$$I(\omega) = \frac{e^2}{3\pi\epsilon_0 c^3} |\dot{\mathbf{v}}(\omega)|^2 \quad (5.34)$$

This is the total energy per unit bandwidth emitted throughout the period of acceleration. for distribution of particles, this result must be integrated over all the particles contributing to the radiation at frequency ω .

5.3.3 Bremsstrahlung

In the 1930s, Carl Anderson found that the ionisation loss rate given by the Bethe-Bloch formula (An improved version of equation (5.1) obtained by a quantum mechanical treatment, which accounts for relativity) underestimates the energy loss rate for relativistic electrons. The additional loss was associated with the radiation emitted by the accelerating electron in the electrostatic field of the nucleus. This radiation was first discovered by Nikola Tesla in the 1880s in a different context, was called 'braking radiation' or, in German, bremsstrahlung. It is also called free-free emission in the language of atomic physics.

The quantum mechanical approach is beyond the scope of this report and thus a classical approach with quantum mechanical parts are added as appropriate. The expression for acceleration of an electron in the electrostatic field of a high energy proton or nucleus has already been covered in the section leading up to equations (5.3). Now the roles of the particles are interchanged, but by symmetry, the field experienced by the electron in its rest frame is exactly the same as before. To work out the spectrum, we first take the Fourier transform of the acceleration of the electron and then with the help of expression (5.34), determine the the radiation spectrum. We then integrate this result over all collision parameters, just as in the case of ionisation losses, and use suitable limits. In the case where the electron is moving relativistically, we convert the result back to laboratory frame.

Firstly we calculate the electrostatic acceleration of the electron in its rest frame in parallel and perpendicular directions of motion, a_{\parallel} and a_{\perp} , using equation (5.3):

$$a_{\parallel} = \dot{\mathbf{v}}_x = -\frac{eE_x}{m_e} = \frac{\gamma Ze^2 vt}{4\pi\epsilon_0 m_e [b^2 + (\gamma vt)^2]^{3/2}} \quad (5.35)$$

$$a_{\perp} = \dot{\mathbf{v}}_z = -\frac{eE_z}{m_e} = \frac{\gamma Ze^2 b}{4\pi\epsilon_0 m_e [b^2 + (\gamma vt)^2]^{3/2}} \quad (5.36)$$

Where Ze is the charge of the nucleus.

Using the Fourier transforms of the accelerations in these equations:

$$\begin{aligned} \dot{\mathbf{v}}_x(\omega) &= \frac{1}{(2\pi)^{1/2}} \int_{-\infty}^{\infty} \frac{\gamma Ze^2 vt}{4\pi\epsilon_0 m_e [b^2 + (\gamma vt)^2]^{3/2}} \exp(i\omega t) dt \\ \dot{\mathbf{v}}_z(\omega) &= \frac{1}{(2\pi)^{1/2}} \int_{-\infty}^{\infty} \frac{\gamma Ze^2 b}{4\pi\epsilon_0 m_e [b^2 + (\gamma vt)^2]^{3/2}} \exp(i\omega t) dt \end{aligned}$$

Changing variables to $x = \gamma vt/b$,

$$\begin{aligned} \dot{\mathbf{v}}_x(\omega) &= \frac{1}{(2\pi)^{1/2}} \frac{Ze^2}{4\pi\epsilon_0 m_e} \frac{1}{\gamma bv} \int_{-\infty}^{\infty} \frac{x}{(1+x^2)^{3/2}} \exp(i\frac{\omega b}{\gamma v} x) dx \\ &= \frac{1}{(2\pi)^{1/2}} \frac{Ze^2}{4\pi\epsilon_0 m_e} \frac{1}{\gamma bv} I_1(y) \\ \dot{\mathbf{v}}_z(\omega) &= \frac{1}{(2\pi)^{1/2}} \frac{Ze^2}{4\pi\epsilon_0 m_e} \frac{1}{bv} \int_{-\infty}^{\infty} \frac{x}{(1+x^2)^{3/2}} \exp(i\frac{\omega b}{\gamma v} x) dx \\ &= \frac{1}{(2\pi)^{1/2}} \frac{Ze^2}{4\pi\epsilon_0 m_e} \frac{1}{bv} I_2(y) \end{aligned}$$

Where $y = \omega b/\gamma v$. The integrals $I_1(y)$ and $I_2(y)$ are

$$I_1(y) = 2iyK_0(y) \quad I_2(y) = 2yK_1(y)$$

where K_0 and K_1 are modified Bessel functions of order zero and one. These are solutions to the modified Bessel's equation: $x^2 \frac{d^2y}{dx^2} + x \frac{dy}{dx} - (x^2 + \alpha^2)y = 0$, where α is the order. K_α is a decaying exponential of the form $K_\alpha(x) = \int_0^\infty e^{-x} \cosh t \cosh \alpha t dt$.

The radiation spectrum of the electron in an encounter with a charged nucleus with collision parameter b is therefore

$$\begin{aligned} I(\omega) &= \frac{e^2}{3\pi\epsilon_0 c^3} [|a_{\parallel}(\omega)|^2 + |a_{\perp}(\omega)|^2] \\ &= \frac{Z^2 e^6}{24\pi^4 \epsilon_0^3 c^3 m_e v^2} \frac{\omega^2}{\gamma^2 v^2} \left[\frac{1}{\gamma^2} K_0^2 9 \frac{\omega b}{\gamma v} + K_1^2 \left(\frac{\omega b}{\gamma v} \right) \right] \end{aligned}$$

The impulse perpendicular to the direction of motion of the electron contributes the greater intensity, even in the non relativistic case. This component results in significant radiation at low frequencies. When the particle is relativistic, the intensity due to acceleration along the trajectory of the particle is decreased by a factor of γ^2 relative to the non-relativistic case. Thus, the dominant contribution to the radiation spectrum results from the momentum impulse perpendicular to the line of flight of the electron.

At high frequencies, there is an exponential cut-off in the radiation spectrum:

$$I(\omega) = \frac{Z62e^6}{48\pi^3 \epsilon_0^3 c^3 m_e^2 v^2} \frac{\omega}{\gamma b v} \left[\frac{1}{\gamma^2} + 1 \right] \exp \left(-\frac{2\omega b}{\gamma v} \right)$$

The duration of relativistic collision is roughly $\tau = 2b/\gamma v$ (from the section on Ionisation losses). Thus the dominant Fourier component of the radiation corresponds to frequencies $\nu \approx 1/\tau = \gamma v/2b$ and hence $\omega \approx \pi\nu\gamma/b$. Thus the order of magnitude of $\omega b/\gamma v \approx 1$. Exponential cutoff means there is little power emitted at frequencies higher than $\omega \approx \gamma v/b$. The low frequency spectrum has the form

$$I(\omega) = \frac{Z^2 e^6}{24\pi^4 \epsilon_0^3 c^3 m_e^2 v^2} \frac{1}{b^2} \left[1 + \frac{1}{\gamma^2} \left(\frac{\omega b}{\gamma v} \right)^2 \ln^2 \frac{\omega b}{\gamma v} \right]$$

In the limit $\omega b/\gamma v \ll 1$, the second term in the square brackets can be ignored and thus a good approximation for the low frequency intensity spectrum is:

$$I(\omega) = \frac{Z^2 e^6}{24\pi^4 \epsilon_0^3 c^3 m_e^2 b^2 v^2} = K$$

This was expected as so far as these frequencies are concerned, the momentum impulse is a delta function, which is to say the duration of collision is much shorter than the period of the waves. The Fourier transform of a delta function is a flat spectrum, a constant. Also note that the factor γ has disappeared from the intensity spectrum in the equation above, even in the relativistic case. This is in agreement with equation (5.7) which says the momentum impulse is same in the relativistic and non relativistic case.

Finally we integrate over all collision parameters which contribute to the radiation at frequency ω . We also need to convert the result to the laboratory frame. If the electron was moving relativistically, the number of nuclei it observes also increases by a factor γ because of relativistic length contraction. Hence in the moving frame of the electron, $N' = \gamma N$ where N is the space density of nuclei in the laboratory frame of reference. The number of encounters per second is $N'v$ since all parameters are now measured in the rest frame of electron and superscript dashes are added to all the relevant parameters. The radiation spectrum in the frame of the electron is therefore

$$I(\omega') = \int_{b'_{min}}^{b'_{max}} 2\pi b' \gamma N v K db' = \frac{Z^2 e^6 \gamma N}{12\pi^3 \epsilon_0^3 c^3 m_e^2 v} \ln \left(\frac{b'_{max}}{b'_{min}} \right) \quad (5.37)$$

Non-Relativistic Bremsstrahlung Energy Loss Rate

In the case of a high energy but non relativistic electron, we can set $\gamma = 1$, drop the dashes on b_{max} and b_{min} and neglect relativistic correction factors. Thus the low frequency radiation spectrum (5.37) becomes

$$I(\omega) = \frac{Z^2 e^6 N}{12\pi^3 \epsilon_0^3 c^3 m_e^2 v} \frac{1}{v} \ln \Lambda \quad (5.38)$$

where $\Lambda = b_{max}/b_{min}$. For b_{max} , we integrate out to those values of b for which $\omega b/v = 1$ to find b_{max} . This is because for larger values of b , the radiation at frequency ω makes a negligible contribution to the intensity. For b_{min} , the expression derived in ionisation losses (equation (5.2)) is used. Thus when $v \leq (Z/137)c$, we consider it to be low velocity and vice versa. This gives the following choices

$$\begin{aligned} \Lambda &= \frac{8\pi\epsilon_0 m_e v^3}{Ze^2 \omega} && \text{for low velocities} \\ \Lambda &= \frac{2m_e v^2}{\hbar\omega} && \text{for high velocities} \end{aligned}$$

The electron cannot give up more than its total kinetic energy in the radiation process and so no photons are radiated with energies greater than $\epsilon = \hbar\omega = \frac{1}{2}m_e v^2$. The full quantum mechanical treatment by Bethe and Heitler (oh) gives

$$I(\omega) = \frac{8}{3} Z^2 \alpha \hbar r_e^2 \frac{m_e c^2}{E} v N \ln \left[\frac{1 + (1 - \epsilon/E)^{1/2}}{1 - (1 - \epsilon/E)^{1/2}} \right]$$

where $\alpha = e^2/4\pi\epsilon_0 c \approx 1/137$ is the fine structure constant and $r_e = e^2/4\pi\epsilon_0 m_e c^2$ is the classical electron radius. The equation contains \hbar , which is usually not an indicator of classical formulae but that \hbar gets cancelled with the one in the fine structure constant's expansion. Thus we can see that the coefficient term to the logarithm is exactly the same as was derived by classical methods and the term in the logarithm simplifies down to the equation for collision parameter at high velocities.

To find the total energy loss rate, we integrate equation (5.38) over all frequencies, which is upto ω_{max} , which is the frequency corresponding to cut-off, $b_{min} \approx \hbar/2m_e v$. This is approximately

$$\omega_{max} = \frac{2\pi}{\tau} \sim \frac{2\pi v}{b_{min}} \approx \frac{4\pi m_e v^2}{\hbar}$$

This is to the order of magnitude $\hbar\omega \sim \frac{1}{2}m_e v^2$. This is the maximum kinetic energy of the electron which can be lost in a single encounter with the nucleus. Thus integrating equation (5.38) from $\omega = 0$ to $\omega = m_e v^2/2\hbar$,

$$-\left(\frac{dE}{dt}\right)_{brems} \approx \int_0^{\omega_{max}} \frac{Z^2 e^6 N}{12\pi^3 \epsilon_0^3 c^3 m_e^2 v} \frac{1}{v} \ln \Lambda \, d\omega \quad (5.39)$$

$$\approx \frac{Z^2 e^6 N v}{24\pi^3 \epsilon_0^3 c^3 m_e \hbar} \ln \Lambda = (\text{constant}) Z^2 N v \quad (5.40)$$

Thus the total loss rate is proportional to v and hence $-dE/dt \propto E^{1/2}$. This however will not be the case in relativistic bremsstrahlung.

Thermal Bremsstrahlung

To work out the spectrum of bremsstrahlung of a thermal plasma at temperature T , the expressions the expression for radiation of a single particle (5.38) should be integrated over the

collision parameters and then over a Maxwellian distribution of electron velocities

$$N_e(v) dv = 4\pi N_e \left(\frac{m_e}{2\pi kT} \right)^{3/2} v^2 \exp \left(-\frac{m_e v^2}{2kT} \right) dv$$

The algebra becomes involved at this stage and is skipped from this report. An approximate expression for the spectral emissivity of a plasma of electron density N_e in the low frequency limit is

$$I(\omega) \approx \frac{Ze^{26}NN_e}{12\sqrt{3}\pi^3\epsilon_0^3c^3m_e^2} \left(\frac{m_e}{kT} \right)^{1/2} g(\omega, T)$$

where $g(\omega, T)$ is known as a Gaunt factor. The low frequency spectrum is more or less independent of frequency as it only depends on the slowly varying Gaunt factor. Detailed calculations give the spectral emissivity of the plasma in terms of frequency ν rather than angular frequency ω as

$$\kappa_\nu = \frac{1}{3\pi^2} \left(\frac{\pi}{6} \right)^{1/2} g(\nu, T) NN_e \exp \left(-\frac{h\nu}{kT} \right) \quad (5.41)$$

At frequencies $h\nu \ll kT$, the Gaunt factor (in terms of frequency, not angular frequency) is given as:

$$\text{Radio : } g(\nu, T) = \frac{\sqrt{3}}{2\pi} \left[\ln \left(\frac{128\epsilon_0^2 k^3 T^3}{m_e e^4 \nu^2 Z^2} \right) - \gamma^{1/2} \right]$$

$$\text{X-ray : } g(\nu, T) = \frac{\sqrt{3}}{\pi} \ln \left(\frac{kT}{h\nu} \right)$$

where $\gamma = 0.577\dots$ is Euler's constant. For frequencies $h\nu/kT \gg 1$, $g(\nu, T)$ is approximately $(h\nu/kT)^{1/2}$.

The total loss rate of the plasma is

$$-\left(\frac{dE}{dt} \right)_{\text{brems}} = 1.435 \times 10^{-40} Z^2 T^{1/2} \bar{g} NN_e \text{ W m}^{-3} \quad (5.42)$$

The averaged value of the Gaunt factor \bar{g} lies in the range $1.1 - 1.5$ and thus a good approximation is $\bar{g} = 1.2$.

It is also important to consider thermal bremsstrahlung absorption corresponding to the emissivity as the resulting spectrum is the signature of compact regions of ionised hydrogen in the radio waveband. Using equilibrium conditions, basic absorption equations and substituting the equation for spectral emissivity (5.41) gives us the expression

$$\chi_\nu = (\text{constant}) \frac{NN_e T^{-1/2}}{\nu^3} g(\nu, T) \left[1 - \exp \left(-\frac{h\nu}{kT} \right) \right] \quad (5.43)$$

where χ_ν is the absorption coefficient.

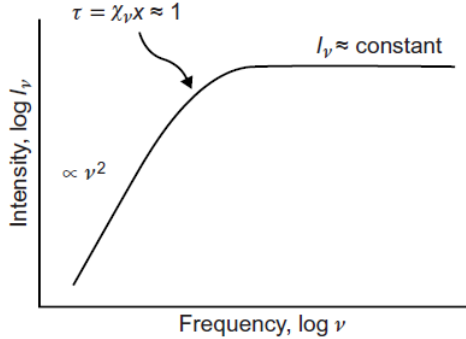


Figure 5.2: The spectrum of thermal bremsstrahlung at low radio frequencies at which self-absorption becomes important. This is the characteristic spectrum of the compact regions of ionised hydrogen found in regions of star formation. [1]

A useful practical result obtained on further analysis is the shape of spectrum of a compact region of ionised hydrogen. This curve is flat with $I_\nu = \text{constant}$ if optical depth (a dimensionless quantity expressing the ratio of incident to transmitted power logarithmically) $\tau \ll 1$ and has a Rayleigh-Jeans thermal spectrum like tail with $I_\nu \propto \nu^2$ if $\tau \gg 1$.

Relativistic Bremsstrahlung

The expression (5.37) is valid as before, but the values of collision parameters b'_{max} and b'_{min} need to be re-evaluated. Since these are linear dimensions perpendicular to the line of flight of the electron, they take the same values in S and S'.

It might be expected that the value of b_{min} should be the same as before, $b_{min} = \hbar/\gamma m_e v$. However in case the electron has 'size' Δx and the duration of the impulse is shorter than the electron's travel time across Δx , the different bits of the probability distribution of the electron need to be considered which may experience the momentum impulse at different times and hence the radiation may not be coherent, which is a problem. Thus the duration of impulse must be at least as long as the time it takes the electron to travel Δx . Thus $\Delta t \geq \Delta x/v$ or

$$\frac{b}{\gamma v} \geq \frac{\hbar}{\gamma m_e v \cdot v} \text{ and hence } b_{min} = \frac{\hbar}{m_e v}$$

To find b_{max} , we can consider the case of neutral atoms interacting with the electron. Using the Fermi-Thomas model of an atom to simplify calculations, the electrostatic potential of the nucleus can be written as

$$V(r) = \frac{Ze^2}{4\pi\epsilon_0 r} \exp\left(-\frac{r}{a}\right)$$

where

$$a = 1.4 a_0 Z^{-1}$$

and a_0 is the Bohr radius of the hydrogen atom. Thus for neutral atoms, a suitable value for b_{max} is $b_{max} = 1.4 a_0 Z^{-1/3}$. In the ultra relativistic limit, $\gamma \rightarrow \infty$, (5.37) becomes

$$I(\omega') = \frac{Z^2 e^6 \gamma N}{12\pi^3 \epsilon_0^3 c^3 m_e^2 v} \ln\left(\frac{1.4 a_0 m_e v}{Z^{1/3} \hbar}\right) \quad (5.44)$$

To transform this to the laboratory reference frame, it can be seen that $I(\omega')$ has the dimensions of energy per unit time per unit bandwidth. In the subsection covering expression (5.8), the

relativistic invariant nature of dE/dt was covered. Thus only the effects on $\Delta\omega$ need to be seen. It is simplest to note that ω transform like E and hence,

$$\Delta\omega = \gamma\Delta\omega'$$

Thus the bandwidth increases and intensity per unit bandwidth decreases by a factor of γ , giving

$$I(\omega) = \frac{Z^2 e^6 N}{12\pi^3 \epsilon_0^3 c^3 m_e^2 v} \ln\left(\frac{192v}{Z^{1/3}c}\right) \quad (5.45)$$

The intensity spectrum is independent of frequency up to energy $\hbar\omega = (\gamma - 1)m_e c^2$, which corresponds to the electron giving up all of its kinetic energy in a single collision. The total loss rate is found by integrating over frequency,

$$-\frac{dE}{dt} = \int_0^{E/\hbar} I(\omega) d\omega$$

Since $v \approx c$,

$$-\frac{dE}{dt} = \frac{Z^2 e^6 N E}{12\pi^3 \epsilon_0^3 c^4 \hbar} \ln\left(\frac{192}{Z^{1/3}}\right) \quad (5.46)$$

Comparing this to the formula derived by Bethe and Heitler from full relativistic quantum treatment

$$-\frac{dE}{dt} = \frac{Z(Z + 1.3)e^6 N}{16\pi^3 \epsilon_0 63m_e^2 c^4 \hbar} E \left[\ln\left(\frac{183}{Z^{1/3}}\right) + \frac{1}{8} \right]$$

it can be seen that despite making many approximations, expression (5.46) is remarkably close to the correct answer.

Notice that in contrast to the non-relativistic case (5.39), the relativistic bremsstrahlung energy loss rate is proportional to the energy of the electron.

5.4 Synchrotron Radiation

The synchrotron radiation of ultra-relativistic electrons dominates much of high energy astrophysics. The radiation is the emission of high energy electrons gyrating in a magnetic field and is the process responsible for radio emission in our galaxy, of supernova remnants and of extragalactic radio sources. It is also the source of non thermal optical emission from the Crab Nebula to possibly X-rays from quasars. A continuum spectrum is said to be 'non thermal' when it cannot be explained by thermal bremsstrahlung or black body radiation.

5.4.1 Dynamics of Charged Particles in Uniform Magnetic Fields

It is necessary to cover the basics of motion of charged particles in magnetic field to understand synchrotron radiation. In the simplest case of a particle of rest mass m_0 , charge ze and velocity \mathbf{v} , corresponding to Lorentz factor $\gamma = (1 - \mathbf{v} \cdot \mathbf{v}/c^2)^{1/2}$ in a uniform static magnetic field \mathbf{B} , the equation of motion is

$$\frac{d}{dt}(\gamma m_0 \mathbf{v}) = ze(\mathbf{v} \times \mathbf{B})$$

On expanding the LHS, we get two terms. However one of them involves a $\mathbf{b} \cdot \mathbf{a}$ which equates to zero as \mathbf{v} is always perpendicular to \mathbf{a} . As a result,

$$\gamma m_0 \frac{d\mathbf{v}}{dt} = ze(\mathbf{v} \times \mathbf{B})$$

Now splitting \mathbf{v} into its components parallel and perpendicular to \mathbf{B} . The parallel component v_{\parallel} does not change due to magnetic forces. The pitch angle θ is defined by $\tan \theta = v_{\perp}/v_{\parallel}$. Thus the acceleration in the direction of $\mathbf{v} \times \mathbf{B}$ is

$$\gamma m_0 \frac{d\mathbf{v}}{dt} = ze |\mathbf{v}| |\mathbf{B}| \sin \theta (\mathbf{i}_v \times \mathbf{i}_B)$$

where \mathbf{i}_v and \mathbf{i}_B are unit vectors in the directions of \mathbf{v} and \mathbf{B} respectively. Because the magnetic field is uniform, this constant acceleration perpendicular to the instantaneous velocity vector and thus results in circular motion about the magnetic field direction. Equating this acceleration to the centripetal acceleration,

$$\frac{v_{\perp}^2}{r} = \frac{ze |\mathbf{v}| |\mathbf{B}| \sin \theta}{\gamma m_0}, \text{ that is, } r = \frac{\gamma m_0 |\mathbf{v}| \sin \theta}{ze |\mathbf{B}|} \quad (5.47)$$

Thus the motion of the particle consists of constant velocity along direction of magnetic field and circular motion with radius r . Thus this signifies a spiral path of constant pitch. The angular gyrfrequency of this motion is

$$\omega_g = \frac{v_{\perp}}{r} = \frac{ze |\mathbf{B}|}{2\pi\gamma m_0}$$

A useful figure to keep in mind is the non relativistic gyrofrequency of an electron at unit magnetic field: $\nu_g = e |\mathbf{B}| / 2\pi m_e = 28 \text{ GHz T}^{-1}$.

Time Varying Magnetic Fields

Instead of the usual physical approach it is helpful to use the principle of action and adiabatic invariant. However, it is not feasible to cover Lagrangian mechanics in this report and thus the mathematical derivation is skipped. Thus some important results are:

- The magnetic moment of a particle is invariant provided the magnetic field is slowly varying. This results in some interesting phenomena such as magnetic mirroring. It follows the expression $\Delta(p_{\perp/B})=0$ which implies that if a particle is moving towards a region of converging magnetic field lines, the magnetic flux density increases and thus perpendicular kinetic energy must also increase. However, the magnetic field does no work and hence this energy needs to come from the kinetic energy due to motion in direction parallel to the field. Given the right conditions, the particle will get reflected back.
- The particle follows the guiding centre in such a way that the number of field lines within the particle's orbit is constant.
- Some more invariants and their results are

$$\Delta(Br^2) = 0 \quad r = \gamma m_0 v_{\perp} / zeB \quad (5.48)$$

$$\Delta(p_{\perp}^2/B) = 0 \quad p_{\perp} = \gamma m_0 v_{\perp} \quad (5.49)$$

$$\Delta(\gamma\mu) = 0 \quad \mu = \gamma m_0 v_{\perp}^2 / 2B \quad (5.50)$$

5.4.2 Synchrotron Total Energy Loss Rate

The electrostatic tools required have already been covered in the previous section. Some important magnetism concepts required are as follows. In a uniform magnetic field, a high energy electron moves in a spiral path at a constant pitch angle α^2 . Its velocity along the field lines is constant while it gyrates about the magnetic field direction at relativistic gyrofrequency

$\nu_g = eB/2\pi\gamma m_e = 28\gamma^{-1}$ GHz T $^{-1}$, where γ is the Lorentz factor of the electron as usual and B is the strength of the magnetic field. The electron is therefore accelerated towards the guiding centre of its orbit and its radiation can be derived from results of expression (5.29). From this equation, the loss rate of a charged particle q with accelerations a_{\perp} and a_{\parallel} as measured in the laboratory frame of reference,

$$-\left(\frac{dE'}{dt'}\right)_{rad} = \frac{q^2\gamma^4}{6\pi\epsilon_0 c^3} [|a_{\perp}|^2 + \gamma^2 |a_{\parallel}|^2]$$

The acceleration is always perpendicular to the velocity vector of the particle and hence from (5.47), $a_{\perp} = evB \sin \alpha / \gamma m_e$ and $a_{\parallel} = 0$. Thus total loss rate is

$$-\left(\frac{dE}{dt}\right) = \frac{\gamma^4 e^2}{6\pi\epsilon_0 c^3} |a_{\perp}|^2 = \frac{\gamma^4 e^2}{6\pi\epsilon_0 c^3} \frac{e^2 v^2 B^2 \sin^2 \alpha}{\gamma^2 m_e^2} \quad (5.51)$$

$$= \frac{e^4 B^2}{6\pi\epsilon_0 c m_e^2} \frac{v^2}{c^2} \gamma^2 \sin^2 \alpha \quad (5.52)$$

We can rewrite this equation by using Thomson cross-section $\sigma_T = e^4/6\pi\epsilon_0^2 c^4 m_e^2$, the energy density of the magnetic field as $U_{mag} = B^2/2\mu_0$ and substituting $c^2 = (\mu_0\epsilon_0)^{-1}$. In the ultra-relativistic limit $v \rightarrow c$, the total loss rate becomes

$$-\left(\frac{dE}{dt}\right) = 2\sigma_T c U_{mag} \gamma^2 \sin^2 \alpha$$

It is important to consider disturbances in the magnetic field causing the pitch angle to change and cause instabilities. Thus averaging over an isotropic distribution of pitch angles $p(\alpha) d\alpha = \frac{1}{2} \sin \alpha d\alpha$, we find the average energy loss rate

$$-\left(\frac{dE}{dt}\right) = 2\sigma_T c U_{mag} \gamma^2 \left(\frac{v}{c}\right)^2 \frac{1}{2} \int_0^\pi \sin^3 \alpha d\alpha = \frac{4}{3} \sigma_T c U_{mag} \left(\frac{v}{c}\right)^2 \gamma^2 \quad (5.53)$$

5.4.3 Non-relativistic Gyroradiation and Cyclotron Radiation

Considering the case of non-relativistic gyroradiation in which case $\gamma = 1$,

$$-\left(\frac{dE}{dt}\right) = \frac{2\sigma_T}{c} U_{mag} v_{\perp}^2 \quad (5.54)$$

and the radiation emitted at the non relativistic gyrofrequency of the electron $\nu_g = eB/2\pi m_e$. In the non relativistic case, there are no beaming effects. When the magnetic field is perpendicular to the line of sight, linearly polarised radiation is observed because the acceleration vector performs simple harmonic motion in a plane perpendicular to the magnetic field direction. The electric field varies sinusoidally at the gyrofrequency as the dipole distribution of radiation sweeps past the observer. If the magnetic field is along the direction of line of sight instead, the light observed will be circularly polarised.

In the case of mildly relativistic cyclotron radiation, beaming cannot be neglected. Here not all of the radiation is emitted at gyrofrequency because of small aberration effects which slightly distort the observed intensity from a $\cos^2 \theta$ law. Using the results of this section it is possible to calculate the magnetic field strength at places such as the poles of a white dwarf, by measuring the fundamental frequency and frequency spacing between separate harmonics of cyclotron radiation. Moreover, using the variation in circular polarisation with orbital phase enable the geometry of the magnetic field configuration to be determined.

5.5 Interactions of High Energy Photons

Three main processes are involved in the interaction of high energy photons with matter: photoelectric absorption, Compton scattering and electron-positron pair production. Except the last (being beyond the scope of this report), these will be covered in this section:

5.5.1 Photoelectric Absorption

At low photon energies, $\hbar\omega \ll m_e c^2$, the dominant mode of interaction between photons and matter is photoelectric. In case of high energy X Rays, they can eject an electron from the atomic energy level E_1 , giving the electron the kinetic energy $(\hbar\omega - E_1)$ once it escapes. For example, the analytic solution for absorption cross section for photons of energies more than enough to liberate electrons but much less than the amount required to produce electron-positron pairs is

$$\alpha_K = \frac{e^{12} m_e^{3/2} Z^5}{192 \sqrt{2} \pi^5 \epsilon_0^6 \hbar^4 c} \left(\frac{1}{\hbar\omega} \right)^{7/2}$$

The absorption cross section has a strong dependence on the atomic number so even though the heavier elements are much rarer, the combination of Z^5 with ω^{-3} means that these heavier elements make significant contributions to the total absorption cross section at X-rays and UV energies. This allows us to determine the abundance of elements in interstellar matter.

5.5.2 Thomson and Compton Scattering

Thomson Scattering

The process of Thomson scattering involves scattering of photons without change in energy, unlike Compton scattering. Thomson used Larmor's formula (5.26) by carrying out a completely classical analysis of the scattering of an unpolarised parallel beam of radiation through an angle α by a stationary electron using the radiation formula (5.24). Without loss of generality, it can be assumed that the beam propagates in positive z direction and scatters in the $x-z$ plane with angle α . The electric field strength of unpolarised incident field is resolved into components of equal intensity with electric vectors in the orthogonal \mathbf{i}_x and \mathbf{i}_y directions (Figure 5.3). The electric fields experienced by the electron in x and y directions will be $E_x = E_{x0} \exp(i\omega t)$ and $E_y = E_{y0} \exp(i\omega t)$ and will cause the electron to oscillate and experience the accelerations

$$\ddot{\mathbf{r}}_x = eE_x/m_e; \quad \ddot{\mathbf{r}}_y = eE_y/m_e$$

Thus using these in (5.24) with $\alpha = \pi/2 - \theta$. The intensity of radiation scattered through angle θ into the solid angle $d\Omega$ is then

$$-\left(\frac{dE}{dt}\right)_x d\Omega = \frac{e^2 |\ddot{\mathbf{r}}_x|^2 \sin^2 \theta}{16\pi^2 \epsilon_0 c^3} d\Omega = \frac{e^4 |E_x|^2}{16\pi^2 m_e^2 \epsilon_0 c^3} \cos^2 \alpha d\Omega$$

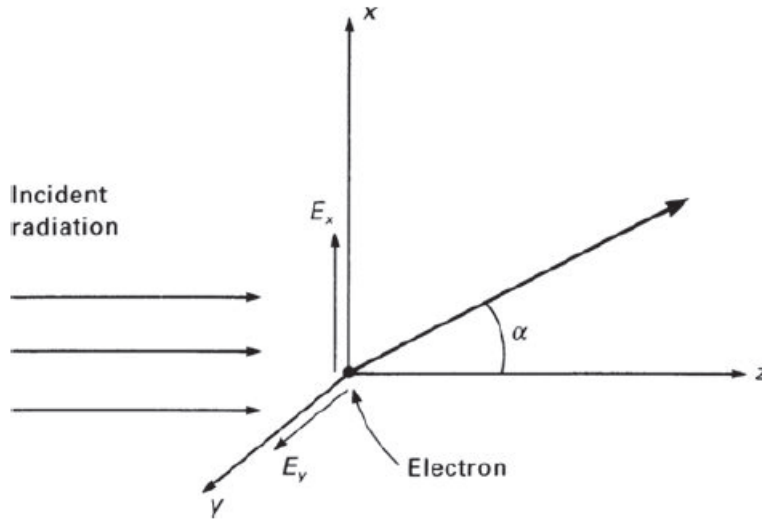


Figure 5.3: The geometry of Thomson scattering of a beam by a free electron. [1]

Taking time averages of E_x^2 , $\bar{E}_x^2 = E_{x0}^2/2$. Summing over all waves contributing to E_x component of radiation and expressing the sum in terms of incident energy per unit area upon the electron. This is given by Poynting's theorem, $\mathbf{S}_x = (\mathbf{E} \times \mathbf{H}) = c\epsilon_0 E_0^2 \mathbf{i}_z$. Since the radiation is incoherent, we use the total intensity in direction α from x component of acceleration as $S_x = \sum_i c\epsilon_0 E^2 - x0/2$ and so

$$-\left(\frac{dE}{dt}\right)_x d\Omega = \frac{e^4 \cos^2 \alpha}{16\pi^2 m_e^2 \epsilon_0 c^3} \sum_i \bar{E}_x^2 d\Omega = \frac{e^4 \cos^2 \alpha}{16\pi^2 m_e^2 \epsilon_0^2 c^4} S_x d\Omega$$

Next considering the scattering of E_y component of the incident field. This will correspond to scattering through $\theta = 90^\circ$ and therefore the scattered intensity in the α direction is

$$-\left(\frac{dE}{dt}\right)_y d\Omega = \frac{e^4}{16\pi^2 m_e^2 \epsilon_0^2 c^4} S_y d\Omega.$$

Thus total scattered radiation into $d\Omega$ is found by adding the intensities of two independent field components,

$$-\left(\frac{dE}{dt}\right) d\Omega = \frac{e^4}{16\pi^2 m_e^2 \epsilon_0^2 c^4} (1 + \cos^2 \alpha) \frac{S}{2} d\Omega$$

Where $S = S_x + S_y$. For unpolarised radiation, $S_x = S_y$. Now expressing the scattered intensity in terms of a differential scattering cross-section $d\alpha_T$ in direction α by

$$\frac{d\alpha_T}{d\Omega} = \frac{\text{energy radiated per unit time per unit solid angle}}{\text{incident energy per unit time per unit area}}$$

Since this total incident energy per unit time per unit area is S , the differential cross section for Thomson scattering is

$$d\alpha_T = \frac{e^4}{16\pi^2 \epsilon_0^2 m_e^2 c^4} \frac{(1 + \cos^2 \alpha)}{2} d\Omega$$

expressing this in terms of classical electron radius $r_e = e^2/4\pi\epsilon_0 m_e c^2$ and integrating over all solid angles,

$$\sigma_T = \int_0^\pi \frac{r_e^2}{2} (1 + \cos^2 \alpha) 2\pi \sin \alpha d\alpha = \frac{8\pi}{3} r_e^2 = 6.653 \times 10^{-29} \text{ m}^2. \quad (5.55)$$

This is Thomson's famous result for total cross section for scattering of electromagnetic waves by stationary free electrons. Some of the results that can be inferred from this are:

- Scattering is symmetric with respect to scattering angle α . Thus as much radiation is scattered backwards as forwards.
- Even for 100% polarised light the cross section for scattering is the same. This is not surprising as it does not matter how the electron is forced to oscillate.
- One distinctive feature of Thomson scattering is that the scattered radiation is polarised, even if the incident beam of radiation is unpolarised. This can be seen intuitively from Figure 5.3 because all the E -vectors of the unpolarised beam lie in the xy plane. Therefore, when the electron is observed precisely in the xy plane, the scattered radiation is 100% polarised. On the other hand, if we look along the z -direction, we observe unpolarised radiation. Hence this is a way of producing polarised radiation from initially unpolarised radiation.
- Thomson scattering is one of the most important processes which impedes the escape of photons from a medium as the energy of the radiation is unchanged. Hence this process can repeat many times.

Compton Scattering

Compton scattering is important in the cases where the energy of photons is closer to $m_e c^2$ in the centre of mass frame of the electron - photon system. This process involves scattering of photons with exchange in energy. Traditionally, the Compton effect is described in terms of the increase in wavelength of the photon. However, if the angles of interaction (before and after interaction) are randomly distributed, the photon is just as likely to lose energy as it is to gain energy.

To work out the statistical scattering cross section for Compton scattering even in the easiest ways requires analysis using four vectors which is involved. Hence for the remainder of the section, a qualitative approach will be followed.

Compton scattering produces no net change in energy of the photons to the first order v/c and it is only to the second order v^2/c^2 that there is a net energy change. It is also necessary to consider quantum mechanical effects only if the centre of momentum frame moves with a velocity close to that of the electron and in this frame the energy of the photon $\gamma \hbar \omega \sim m_e c^2$.

It is of particular interest to study the effects of inverse Compton scattering because there are certainly electrons with Lorentz factors $\gamma \sim 100 - 1000$ in various types of astronomical sources and they scatter any low energy photons to very much higher energies. For example, Radio photons can be scattered as ultraviolet photons, far infrared photons can produce X-ray photons and optical photons may even produce γ -ray photons. It also provides a mechanism for the inevitable drain of energy of high energy electrons when they pass through regions of large density of radiation.

Qualitatively speaking, the finite electron mass leads to recoil and cause traditional scattering and this increases with photon frequency, while the random electron velocities produce random Doppler shifts of the scatterers in the Laboratory frame and this increases with electron energy.

Chapter 6

High Energy Astrophysics

6.1 Interstellar Gas

The study of interstellar medium is extremely important as not only does it account for some interesting phenomena, but it also affects data collected from faraway sources. The interstellar medium affects stellar evolution from birth to death. Some of the important roles played by interstellar gas are the formation of stars in dense regions and acting as fuel for active galactic nuclei.

The mass of the interstellar medium gas amounts to about 5% of the gas of the visible mass of our galaxy. In our solar neighbourhood in the milky way, the overall gas density is about 10^6 particles m^{-3} .

6.1.1 Neutral Interstellar Gas

The neutral interstellar gas results in a variety of absorption and emission lines across the electromagnetic spectrum. Usually, however, this gas is transparent to light in longer wavelengths such as radio waves. Two interesting aspects of radio lines from interstellar medium are the 21-cm line of emission and absorption caused by the hyperfine transitions in neutral hydrogen and molecular radio lines, the latter being discussed below.

Long before radio astronomy, optical spectral lines for molecules like CH, CH^+ and CN were observed in bright stars. The advantage of observing at radio wavelengths is that there is no interstellar dust extinction. Molecules can emit radiation associated with:

- Electronic transitions: These produce optical light.
- Vibrational transitions: These produce infrared light on the principle of considering molecules as simple harmonic oscillators
- Rotational Transitions: These produce light at radio wavelengths. The different energy levels of rotational motion are based on the quantisation of angular momentum \mathbf{J} such that $\mathbf{J}^2 = j(j+1)\hbar^2$ where $j = 0, 1, 2, \dots$

Using $E = J^2/2I$ where I is the moment of inertia,

$$h\nu = E(j) - E(j-1) = j\hbar^2/I$$

For molecules, $I = \mu r_0^2$ where μ is the reduced mass of the molecule and r_0 is the equilibrium spacing of nuclei. This gives

$$\nu = \frac{j\hbar}{4\pi^2\mu r_0^2} \propto j$$

Thus the spacing between energy levels of rotational transitions is equal and this gives it the name rotational ladder.

6.1.2 Ionised Interstellar Gas

There are many processes by which ionised interstellar gas emits and absorbs radiation, such as thermal Bremsstrahlung radiation, which has been covered in section 5.3.3. This radiation is observed from many sources at different wavelengths, such as at very low radio wavelengths in the Galactic plane to X-ray wavelengths from supernova remnants and intergalactic gas in rich clusters of galaxies. Some other important processes are covered below.

Permitted and Forbidden Transitions in Gaseous Nebulae

Strong emission lines are observed from high-density regions of the interstellar gas which are excited by the ultraviolet emission of hot stars. Mechanism of heating and ionising is photoionisation and photoexcitation, as was covered in section 5.5.1. It can be shown that ionisation is due to photoionisation as $T_{gas} \approx T_*$ where T_* is the temperature of stellar atmosphere, about 5000 – 20000 K, which is much less than the 10^5 K ionisation temperature.

In nebulae of $T_e \approx 5000 - 20000$ K, collisions may only excite electrons to a few levels above ground state. Due to low plasma density, multiple electrons may get excited to these higher energy states and form metastable states. These electrons produce forbidden lines while falling back to the ground state.

Faraday Rotation of Linearly Polarised Radio Signals

Partially ionised plasma on interaction with the galactic magnetic field forms a magnetoactive medium. Under typical conditions of such kind, the electric vector of linearly polarised light is rotated on propagating along the magnetic field direction. This is known as Faraday rotation.

In addition to the rotation of the plane of polarisation, radio emission is depolarised with increasing wavelength. This is because at long wavelengths, there is substantial rotation of the plane of polarisation throughout the region, the polarisation vectors originating from different depths within the region add up to different angles. This is known as Faraday depolarisation.

6.1.3 Overall Picture of Interstellar Gas

Most of the gas in the galaxy is confined to the galactic plane and moves in circular orbits about the galactic centre, the inward gravitational pull being balanced by centrifugal forces. The movement is dictated by distribution of stars and dark matter in the galaxy. The rotational velocities are remarkably constant over radial distances from 3 – 15 kpc, which is inconsistent with both rigid body rotation ($v \propto r$) and Keplerian orbits ($v \propto r^{1/2}$). This provides evidence for dark matter.

Gravitational potential by stars and dark matter aren't enough to explain clumping of gas in giant molecular clouds in the vicinity of spiral arms. Some mechanisms proposed to explain their formation are density wave theory of spiral arms and supernova explosions.

The density wave theory of spiral structure is based upon considerations of the stability of a differentially rotating disk of stars to axial perturbations.

Names	Main constituent	Detected by	Volume of interstellar medium	Fraction by mass	N (m^{-3})	Temperature (K)
'Molecular clouds'	H ₂ , CO CS, etc	Molecular lines. Dust emission	~0.5%	40%	$\geq 10^9$	10–30
'Diffuse clouds'	H, C, O with some ions,	21-cm emission & absorption	5%	40%	$10^6\text{--}10^8$	80
'H I clouds'	C ⁺ , Ca ⁺					
'Cold neutral medium'						
'Intercloud medium'	H, H ⁺ , e ⁻ Ionisation fraction 10–20%	21-cm emission & absorption H α emission	40%	20%	$10^5\text{--}10^6$	8000
'Coronal gas'	H ⁺ , e ⁻ Highly ionised species, O ⁵⁺ , C ⁺³ , etc	O VI Soft X-rays 0.1-2 keV	~50%	0.1%	$\sim 10^3$	$\sim 10^6$

Figure 6.1: Principal phases of interstellar gas. [1]

Heating Mechanisms

The hottest gas is produced in supernova explosions. A shockwave propagates ahead of the supersonically expanding shell of cooling gas and heats the interstellar gas to a high temperature.

A second important heating mechanism is the ultraviolet radiation of young stars. The youngest remain embedded in the cloud they were formed in. The gas temperature is determined by balance of photoionisation and recombination, resulting in a temperature of typically 10^4 K.

Some other mechanisms are intergalactic ionising UV and mass loss from stars.

Cooling Mechanisms

For very hot gases ($> 10^7$ K), bremsstrahlung is the principal cooling mechanism. At lower temperatures (10^4 – 10^7 K), bound bound and bound free transitions of H, He and heavy elements. At yet lower temperatures, the line spectra of heavy elements and lower forbidden line transitions are the dominant phenomena.

It is hence easy to infer that the interstellar medium is far from static. yet it is natural to assume that the principal components listed in table ?? should be in appropriate pressure equilibrium.

6.2 Dead Stars

Stellar death results in many of the high energy phenomena in the universe. Thus it is of utmost importance to study these impressive events. There are many different possibilities here - not all stars die the same. A star is called 'dead' when it stops nuclear fusion and can't do it any further unless fuel is added externally. For massive stars, there are two main ways by which the remnants avoid collapse under their own gravity by replacing the pressure provided by fusion energy:

- White Dwarfs: These are stars that avoid core collapse by electron degeneracy pressure.
- Neutron Stars: These are stars that avoid core collapse by neutron degeneracy pressure.

Degeneracy pressure from electrons or neutrons is caused by a combination of Heisenberg's uncertainty principle and Pauli's exclusion principle for fermions. This will be covered in more detail in a deeper look into these degenerate stars.

6.2.1 Sirius B

It is interesting and helpful to follow the history of the observational discoveries of dead stars, and the conclusions drawn by astrophysicists from the data. It started in the early 19th century when after centuries of trying to observe the motion of the stars relative to each other, Bessel discovered that Sirius was wobbling back and forth every 50 years. He achieved this by using the world's best telescope of the time, designed by Fraunhofer, which was specially built for this purpose as it could numerically measure (in arbitrary units) the movement of the stars over time. He concluded that it must have a massive but invisible companion.

Using simple Newtonian mechanics Bessel figured out the mass and separation of the companion by using the orbital period and mass of Sirius. In this case, the companion star, now called Sirius B, turned out to have a mass of roughly one solar mass.

Upon later observations (with better telescopes), Sirius B was directly observed. It is around 1000 times fainter than the main star (now called Sirius A), despite having half its mass. However spectroscopy also shows that it is 2.5 times hotter than Sirius A.

Using the Stefan-Boltzmann equation for luminosity,

$$L = A\sigma T^4 \quad (6.1)$$

where A is the surface area, σ the Stefan-Boltzmann constant (equal to 5.67×10^{-8} in SI units) and T is the temperature (in K). Comparing it to Sirius A by the formula

$$r_B = r_A \sqrt{\frac{L_B}{L_A}} \left(\frac{T_A}{T_B} \right)^2$$

which comes out as 6000 km. That is even smaller than the earth, yet weighs about as much as the sun. From the expression (3.4), it also has a very high pressure at the centre.

6.2.2 White Dwarfs

The spectra of white dwarfs shows a lack of hydrogen, which is unsurprising as at such high temperatures and pressures you'd expect it to burn up pretty quick. As already mentioned, the collapse of these extreme stars is prevented by electron degeneracy pressure. According to the Pauli's Exclusion Principle, two fermions cannot occupy the same quantum state - the same position and momentum (roughly speaking, in this case). To calculate the degeneracy pressure, the Heisenberg's Uncertainty relation is considered first

$$\Delta x \Delta p \approx \hbar$$

The number of electrons per unit volume = $n_{e \text{ tot}}/\text{Vol}$ but also = $1/(\text{Volume occupied by one electron})$. Hence

$$(\Delta x)^3 n_e = 1 \quad (6.2)$$

$$\Delta x = n_e^{1/3} \quad (6.3)$$

$$\Delta p = \hbar n_e^{1/3} \quad (6.4)$$

Using the approximation $p \approx \Delta p$ and Newton's second law, $F = dp/dt$.

Consider a cube of side 1 m. Then the pressure will be force on one side. Since 1/6th of the electrons will hit one side and total number of electrons = $n_e \text{ Vol} = n_e v \text{ area} = n_e v$ where v is the velocity (since these electrons need to reach the side in one second) and area is unity. Thus

$$P = \frac{1}{6} n_e v \times 2p$$

Here $2p$ is the change in momentum of each electron on collision. Thus substituting $v = p/m_e$ and expression (6.4), and $n_e = \frac{Z}{A} \frac{\rho}{m_H}$ where Z and A are the atomic number and atomic mass respectively (as white dwarfs are mostly made of carbon or oxygen), ρ is the density and m_H is the mass of hydrogen. This gives the approximate result

$$P = \frac{\hbar^2}{3m_e} \left[\left(\frac{Z}{A} \right) \frac{\rho}{m_H} \right]^{5/3}$$

This result is off by approximately a factor of 5 but has the correct features. A more rigorous calculation considering a more realistic (but still non relativistic and thus valid for low masses. The reason for this will be clear soon) case gives the result

$$P = \frac{(3\pi^2)^{2/3}}{5} \frac{\hbar^2}{m_e} \left[\left(\frac{Z}{A} \right) \frac{\rho}{m_H} \right]^{5/3} \quad (6.5)$$

Setting this expression equal to the expression (3.4), an expression for the radius of a white dwarf is obtained:

$$R_{WD} = \frac{(18\pi)^{2/3}}{10} \frac{\hbar^2}{Gm_e M_{WD}^{1/3}} \left[\left(\frac{Z}{A} \right) \frac{1}{m_H} \right]^{5/3} \quad (6.6)$$

Where M_{WD} is the mass of white dwarf. Remarkably, this approximate expression gives a result correct to within a factor of two. It is interesting to note that the radius of a white dwarf is inversely proportional to (the cube root of) the mass of the white dwarf. Thus as the mass of a white dwarf increases and its radius decreases at the same time, the degenerate electrons must reach higher momentum states as the position states were filled already. Due to this, we need to consider a relativistic degenerate gas at higher masses which will affect the equations considerably.

However, there is also the problem of the source of white dwarfs. Their complete lack of Hydrogen and Helium is perplexing as most of the universe is made up of these two elements. The answer lies in events of the class novae, particularly in dwarf novae.

6.2.3 Dwarf Novae

Dwarf novae were first observed in 19th century when certain stars occasionally became 100 times brighter. When the spectra of these stars were taken, it was found that they showed emission lines when faint, but during their explosions, they showed absorption lines.

To explain this strange phenomenon, we look at how matter and radiation interact. If a cloud of gas is tenuous, it will be 'optically thin' and be more likely to give emission lines in the spectrum. On the other hand, an 'optically thick' cloud will show a black body spectrum, given by the Planck law:

$$f_\lambda = \frac{2\pi hc}{\lambda^5 e^{hc/\lambda kT}}$$

where f_λ is the flux per unit wavelength λ and k is Boltzmann's constant. The peak of this spectrum is given by Wein displacement law:

$$\lambda = \frac{0.00290}{T}$$

Integrating the Planck law over all wavelengths gives the Stefan-Boltzmann equation, expression (6.1). Thus if there's a cool gas in front of a black body, it will cause absorption lines. This cooler gas can also be a part of the same object - like the atmosphere of a star.

Thus we can say that the gas in a dwarf nova is optically thin while quiet, but becomes thick (but surrounded by cooler gas) during an eruption.

Looking at the spectrum more closely, the spectrum of a red star along with the gas is seen. The way these spectra oscillate indicate that they are orbiting each other and have roughly the same mass. Balancing the gravitational force with the centrifugal force, it was found that they orbit only a couple of million kilometers apart - almost touching!

Observing the spectrum in yet more ways to see the effect of eclipses, it is found that the gas cloud has at least two bright point like objects inside it. However one of these bright sources shines in only one direction and is flickering. The final clue is that the spectrum of the gas shows two peaks - indicating a rotating gas as the two sides of the rotating gas have opposite Doppler shifts and will show different peaks.

Finally we consider the following physical model: A red star and a white dwarf in orbit around their common centre of mass. The red dwarf is swelling up and its gas is spilling over onto the white dwarf. This can be seen clearly through the means of a Roche surface: a diagram of the potential energy of the system at each point joined by contour lines.

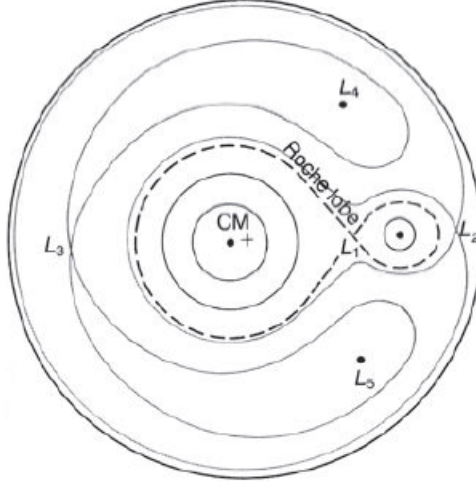


Figure 6.2: Roche Surface showing potentials through contour lines. [1]

Figure 6.2 shows some of the Lagrangian points of stability. If a star becomes so large that some of its volume crosses over the L1 Lagrangian point, it starts losing the gas beyond this point to the white dwarf. This gas then forms a disk around the white dwarf due to its angular momentum.

6.2.4 Accretion Disks

The spinning disk of gas around the white dwarf gets its power from the gravitational potential energy in orbit around the white dwarf as it moves closer to the centre. In the disk, by Kepler's laws, the gas at different radial distances move at different speeds and thus heat up and slow down due to dynamical friction. The power radiated can be calculated from the energy lost and comes out as:

$$P = \frac{GM_{WD}\dot{m}}{r_{WD}}$$

where \dot{m} is the rate of mass transfer, M_{WD} and r_{WD} are the mass and radius of the white dwarf respectively. This can be obtained simply by finding the difference in potential energy of the gas per unit time when it reaches the surface of the white dwarf from the companion star, the latter quantity being ignored due to being large. Using the observational power, the rate of mass transfer comes out around $3 \times 10^{13} \text{ kg s}^{-1}$, which is a tiny fraction of the red star mass. This means the transfer can continue for a very long time.

Using these values we can estimate the temperature of the accretion disk, by making the approximation that it has a uniform temperature. This is given by combining the Power equation and Stefan-Boltzmann equation:

$$T = \sqrt[4]{\frac{GM_{WD}\dot{m}}{\pi r_D^2 r_{WD} \sigma}}$$

where r_D is the disk radius. This comes out as roughly 9000 K. However in practice, the inner part of the disk is much hotter and dominated the spectrum and total emission.

A special case of this is magnetic white dwarfs, where near the surface the accretion disk stops and is funneled into the polar caps of the white dwarf. The charged particles doing spirals around the magnetic field lines can produce synchrotron radiation.

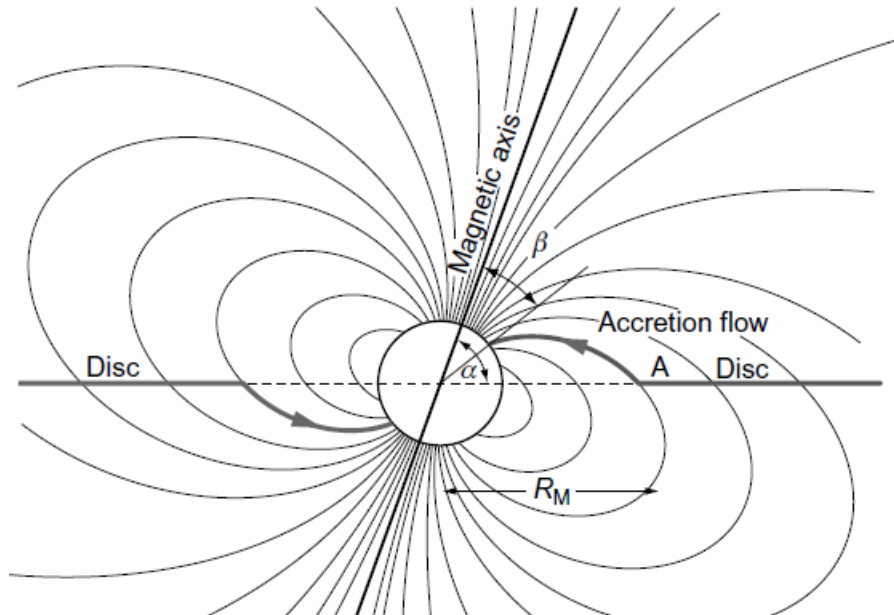


Figure 6.3: Illustrating the accretion of matter from an accretion disc onto the polar caps of a magnetised neutron star or white dwarf. Within the magnetically dominated region, the matter is channelled down the magnetic field lines onto the magnetic poles of the neutron star where its binding energy is released, resulting in strong heating of the plasma. A hot accretion column is formed above the magnetic poles from which intense X-radiation is emitted. [1]

These dwarf novae are very common. Most stars are binaries, and the more massive star will die first and swell up. At this point, tidal drag often brings the two stars close together. The more massive star then turns into a white dwarf, and at some later stage the less massive star begins to swell up. At that point, a dwarf nova is formed. The second flickering source of light observed in the spectrum from earlier is explained by the point of stellar gas joining the accretion disk, which is quite variable and radiates in one side only.

6.2.5 Classical Novae and the Chandrasekhar Limit

Classical novae are explosions much brighter than the dwarf nova explosions. They too repeat, but over much longer timescales. Unlike dwarf novae, these actually blow material out into space. Curiously, some of the classical novae have subsequently turned into dwarf novae, indicating that these too involve binary systems of a red star transferring mass to a white dwarf companion. In this case the energy source is fusion, not gravity. As gas falls on the surface of the white dwarf, a thin shell of hydrogen builds up on the surface.

Since the pressure on the surface of these massive but compact stars is extremely high, fusion can occur on the surface. However, unlike normal stars where fusion causes increase in temperature and consequently pressure, decreasing the density of the star, the pressure in a white dwarf is independent of temperature - it is caused by degeneracy, a quantum mechanical effect. Thus in this case the temperature rises but pressure and density don't change appreciably, causing a runaway reaction that ends in an explosion. This creates all sorts of radioactive elements at the surface which radiate away their energy.

Eddington Limit

From the nuclear explosion, a flood of photons pour out. These can give an electron a push if they come close enough to one to be within its Thomson Cross section (expression 5.55), which has a value $\sigma_T = 6.7 \times 10^{-29} \text{ m}^2$. Thus the cumulative force of all the photons with momentum E/c flooding out from an object of luminosity L and hitting one electron at a distance D is

$$F = \frac{L}{4\pi D^2 c} \sigma_T$$

If this is greater than the force of gravity, the radiation will blow matter out into space. The limiting condition is called the Eddington Luminosity L_E and a classical nova exceeds this limit:

$$L_E = \frac{4\pi G M_{WD} m_p c}{\sigma_T}$$

Chandrasekhar Limit

As was previously discussed, the radius of a white dwarf decreases with mass. As it moves in, the pressure pushes back harder but at the same time, gravity becomes stronger. Thus it is important to look at the balance in these forces to understand the evolution of white dwarfs. Considering the degenerate matter to follow ideal gas law for some process (not isothermal), the expression $PV = c^\gamma$ can be considered for some value of γ . Thus

$$\begin{aligned} P &\propto R^{-3\gamma} \\ F_{\text{pressure}} &\propto R^2 \times R^{-3\gamma} \end{aligned}$$

Meanwhile force due to gravity is proportional to R^{-2} . Thus for $\gamma > 4/3$, the star is stable while for $\gamma \leq 4/3$, it is unstable.

For a normal white dwarf, $\gamma = 5/3$ so the star is stable. However at higher masses, γ tends to

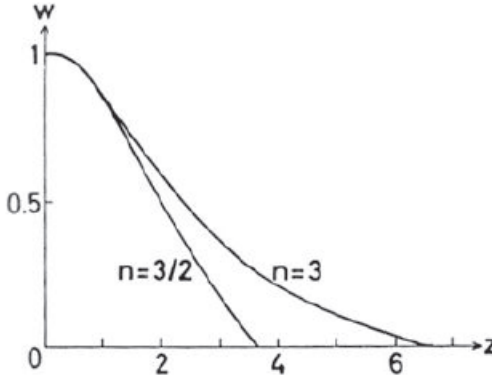


Figure 6.4: Solutions to the Lane Emden equation for polytropic index $n = 3/2$ and 3 . [1]

$4/3$ making it unstable. This is because at higher masses, the pressure at centre of white dwarf obtained from Fermi-Dirac distribution considering the relativistic case,

$$P = \frac{(3\pi^2)^{1/3} \hbar c}{4} \left[\left(\frac{Z}{A} \right) \frac{\rho}{m_H} \right]^{4/3} \quad (6.7)$$

The mass at which γ reaches $4/3$ is called the Chandrasekhar mass. Here it is worth looking into the basis of this in a bit more detail.

Because the pressure is independent of the temperature for degenerate stars, we only need the first two equations of stellar structure (3.7) to carry out the analysis,

$$\frac{dp}{dr} = -\frac{GM\rho}{r^2}; \quad \frac{dM}{dr} = 4\pi r^2 \rho$$

Eliminating M , a second order differential equation relating p and ρ is obtained,

$$\frac{d}{dr} \left(\frac{r^2 dp}{\rho dr} \right) + 4\pi G \rho r^2 = 0 \quad (6.8)$$

As seen in equations (6.5) and (6.7), the pressure depends upon density as $p = \kappa \rho^\gamma$ with $\gamma = 5/3$ and $4/3$ in the non relativistic and relativistic cases. Writing this in terms of polytropic index n such that $\gamma = 1 + (1/n)$. Thus $n = 3/2$ and 3 in the non relativistic and relativistic cases. Now to simplify calculations, we can use some substitutions. Writing the density at any point in the star in terms of density at centre as $\rho(r) = \rho_c \omega^n$. Then writing distance r from centre in terms of dimensionless distance z ,

$$r = az \quad \text{where } a = \left[\frac{(n+1)\kappa \rho_c^{(1/n)-1}}{4\pi G} \right]^{1/2}$$

Using these substitutions, (6.8) becomes

$$\frac{1}{z^2} \left[\frac{d}{dz} \left(z^2 \frac{d\omega}{dz} \right) \right] + \omega^n = 0 \quad (6.9)$$

This is known as the Lane-Emden equation.

Analytic solutions only exist for $n = 0, 1$ and 5 . For values of n less than 5 , the density goes down to 0 at some finite radius z_n which corresponds to the surface of the star at radius $R = az_n$. Using the numerical solutions of z at which ω goes to 0 and substituting in the equation for the definition of a ,

$$\rho_c \propto R^{2n/(1-n)} \quad (6.10)$$

Now the mass-radius relation is found by integrating the density distributions as shown in Figure 6.4 from $r = 0$ to R :

$$\begin{aligned} M &= \int_0^R 4\pi\rho r^2 dr = 4\pi\rho_c \int_0^R \omega^n r^2 dr \\ &= 4\pi\rho_c a^3 \int_0^{z_n} \omega^n z^2 dz = 4\pi\rho_c \left(\frac{r}{z}\right)^3 \int_0^{z_n} \omega^n z^2 dz \end{aligned}$$

But from (6.9),

$$\int_0^{z_n} z^2 \omega^n dz = - \left(z^2 \frac{d\omega}{dz} \right)_R$$

Thus,

$$M = 4\pi\rho_c \left(\frac{R}{z_c}\right)^3 \left[-z^2 \left(\frac{d\omega}{dz}\right) \right]_R \quad (6.11)$$

For any polytrope, the expression in square brackets in (6.11) is a constant for a fixed value of n . The figures quoted by Kippenhahn and Weigert for $-z^2(dw/dt)|_R$ are 2.71406 if $n = 3/2$ and 2.01824 if $n = 3$. Therefore, from (6.10),

$$M \propto \rho_c R^3 \propto R^{(3-n)/(1-n)} \quad (6.12)$$

Thus in the non relativistic case, the greater the mass of the star, the smaller the radius. Consequently as the mass increases until a critical density is reached and the relativistic equation of state with $n = 3$ needs to be considered. At this point from (6.12) it is clear that the radius of a relativistic degenerate star is independent of its mass. Using (6.11) in the relativistic case,

$$M = 2.018244 \times \pi \left(\frac{\kappa}{\pi G}\right)^{3/2} = \frac{(3\pi)^{3/2}}{2} \left(\frac{\hbar c}{G}\right)^{3/2} \times \frac{2.018244}{(\mu_e \mu_u)^2} = \frac{5.836}{\mu_e^2} M_o$$

Where μ is the average mass per free particle denoted in the subscript. In a white dwarf, the limiting mass if expected to correspond to $\mu_e = 2$. Therefore,

$$M_{Ch} = 1.46 M_o$$

This is the famous Chandrasekhar mass.

A few ways by which a white dwarf may get this big is by white dwarf merger or gradual buildup of mass over many cycles of novae. However, they are never formed this massive as even stars with upto 7 times the mass of the sun leave white dwarfs of about $1.2 M_o$. After crossing the Chandrasekhar mass limit, the white dwarf will start to fuse carbon and oxygen to heavier elements. This is an explosive process - even more so than classical novae!

6.2.6 Supernovae

When a white dwarf of carbon and oxygen starts fusing these elements to iron, the total energy converted is around 10^{45} J. This is a massive amount of energy, which can outshine entire small galaxies at optical wavelengths, and forms its own class of novae - supernovae.

Historical records show about four supernovae observed by humanity in the past 1000 years. When these were observed with proper telescopes, the remnants turned out to be expanding shells of gas, so evidence that these bright ‘new stars’ really were explosions. In fact, Fritz Zwicky figured out that if he surveyed enough galaxies with a telescope with a wide field of view, he could find a new supernova every year.

Type	Characteristics
	Type I – absence of hydrogen lines in optical spectrum
Type Ia	Absence of hydrogen lines in spectrum; singly ionised silicon Si II at 615.0 nm observed near peak light.
Type Ib	Neutral helium (He I) line at 587.6 nm observed but no strong silicon absorption feature at 615.0 nm.
Type Ic	Helium lines are weak or absent; no strong silicon absorption feature 615.0 nm.
	Type II – hydrogen lines present in optical spectrum
Type IIP	Reaches a ‘plateau’ in its light curve.
Type IIL	Displays a linear decrease in its light curve
Type IIn	These supernovae contain relatively narrow features compared with the usual broad emission lines of Type II supernovae.
Type I Ib	These supernovae have spectra similar to Type II at early times but to Type Ib/c at later times.

Figure 6.5: Table showing types of supernovae. [1]

As seen in table 6.5, Type 1 supernovae show no hydrogen in their spectra. Since white dwarfs have little or no hydrogen, they might be a good source of these. These supernovae also seem to not show any preference to star forming regions and thus probably originate from the older stellar population.

Type 1 Supernovae

Looking at the nuclear physics involved, most of the carbon and oxygen will fuse to ^{56}Ni . Not much energy is released in this process. The energy is released later, as the ^{56}Ni decays to ^{56}Co (half-life of 6.1 days, releases 1.7 MeV per nucleon) and then this ^{56}Co decays to ^{56}Fe (half life of 77 days, releases 3.7 MeV per nucleon).

Calculating the ^{56}Ni produced from these by observing the peak brightness and observing its total energy, it is seen that only about 10^3 kg of ^{56}Ni is produced - about half a solar mass. This is curiously small as it is less than even half of a Chandrasekhar mass white dwarf. Another unexpected observation from the spectrum is that the it is dominated by lines of calcium, silicon and oxygen. A ‘P Cygni’ profile is obtained which has been covered in section 3.5.1. The lines are very wide due to the enormously high velocities of the outflowing gas.

After a few months, however, the spectrum looks quite different and shows the strong expected lines of iron. So the iron (from the decay of nickel 56) is there, but buried below lots of lighter elements. This can be explained by considering the outer layers which move faster and are beamed at us contain lighter elements while the inner layers of lower velocities contain iron. This means white dwarfs are valid candidates for supernova explosions, but need to be only partially degenerate before the explosion begins.

This can be explained by three models:

- A merger of white dwarfs, which may be a messy process and the Chandrasekhar mass may be crossed by the combined object at the same time as the merger

- Mass could be added slowly to the white dwarf from its binary companion and cause it to start simmering rather than exploding away in a matter of seconds, partially removing the degeneracy.
- The companion star could supply helium, which being a boson does not become degenerate and detonate in a helium flash sending a shock wave to the centre. The compression caused by the shock wave could tip over the core to start fusing despite the white dwarf being under the Chandrasekhar limit.

None of these models completely fit as the remnant is spherically symmetric, which is not expected of the merger model, but there is no sign of the companion star in the spectrum either. One possible explanation for this could be that despite crossing the Chandrasekhar mass, a white dwarf may avoid collapse for a few million to even billion years due to very high spin reducing the pressure on the surface. This way, the companion star may have time to become a white dwarf itself and be too faint to observe in the explosion.

Type 1a supernovae are vital for cosmology as their standard luminosities mean they can be used to measure distances very accurately. In fact, they played a major role in the discovery of dark matter and even cosmological redshift as the 2011 Nobel Prize was awarded to Adam Riess and Brian Schmidt “for the discovery of accelerating expansion of the universe through observations of distant supernovae”.

Type 2 Supernovae

Luckily for astronomers, a type 2 supernova explosion was observed in the Magellanic clouds in 1987. It was extensively studied and observations show that the source of this was a massive star - around 15 times the mass of the sun.

The explosion of massive stars occurs in an entirely different way. These stars can continue to fuse carbon and oxygen to silicon and further to iron and nickel in their cores the normal way in only a few weeks. Once their cores are made of iron and nickel, fusion stops. Gravity takes over and causes the cores to shrink. The cores are too massive to end up as iron-nickel white dwarfs, so they shrink further still.

Their shrinking is finally stopped by neutron degeneracy pressure. This is exactly the same quantum-mechanical effect we discussed when caused by electrons in white dwarf stars, but because neutrons are more massive, they can exert more pressure, and hence support more massive cores. If we take the equation for the radius of a white dwarf, and replace the mass of an electron with the mass of a neutron (1840 times larger), we get a radius 1840 times smaller - i.e. around 3 km. In fact, the cores supported by neutron degeneracy pressure (which are called neutron stars) are around 10km in size.

If the core forms a neutron star, the rest of the star will fall onto this core in the absence of any appreciable outward radiation pressure from the core. Roughly speaking, this process releases energy equal to

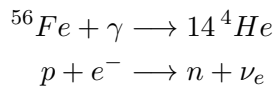
$$E = \frac{GM_{NS}M_S}{r}$$

where M_{NS} is the mass of the neutron star, M_S is the mass of the rest of the star and r the radius of the neutron star. This energy comes out as around 2×10^{47} J - more than 1000 times greater than a type 1 supernova! However it is not straightforward to understand how this fall causes such an explosion. After all, lots of matter is ejected in these supernovae, while normally matter bouncing from a surface usually does not even reach its previous height.

A possible solution is that the star collapses from the inside out. Inner layers bounce off the neutron star and relatively slow speeds, while higher levels bounce off the inner layers (which are already moving out). This can, at least in principle, lead to a tiny fraction of the mass flying out at enormous velocities. But only a small fraction of the energy can be released this way.

Observations show that energy liberated as radiation accounts for around 10^{42} J while the kinetic energy of outflowing matter accounts for around 10^{44} J of energy. This accounts for less than 0.1% of the expected energy.

Looking at the core collapse in more detail, the following inferences are made. As the density increases, the temperature rises to around 10^{10} K. At these temperatures, the black body photons are gamma rays, with enough energy to rip the iron and nickel nuclei apart, breaking them down into their component protons and neutrons, reversing in a fraction of a second all the fusion over the whole lifetime of the star. They follow the reactions



Under these conditions, the electrons and protons combine to produce neutrons and neutrinos. Around 10^{57} neutrinos are produced this way, which are more than enough to account for the expected energy. Even the astounding number of in-falling atoms from the rest of the star only interact with about 1% of the neutrinos (due to the tiny interaction cross section area of around 10^{-47} m²), ejecting out a massive number of particles causing the explosion, while the rest carry the expected energy into space.

From supernova 1987A, a whopping 3×10^{13} neutrinos reached the earth... per meter square! This was enough to get a handful of detections in neutrino detection tanks on earth.

There is still a lot to understand in this process as simulations including all this physics generally tend to stall instead of producing explosions. Observational data also suggests that stars in the mass range 8.5 - 16.5 solar masses explode. This leaves a lot of stars which are even more massive which don't seem to produce supernovae. Full observations will find rarer type of supernovae .

6.2.7 Neutron Stars

Neutron stars are quite similar to white dwarfs if you replace the degenerate electrons with degenerate neutrons. Thus most of the results obtained for white dwarfs are somewhat approximately valid. If the mass of neutron is substituted in place of mass of electron in expression (6.6), then the radius of a neutron star of about 1.5 times the mass of the sun will have a radius of the order of 10 km. This must mean they have absolutely amazing gravity.

However the error due to approximations is greater in case of Neutron stars from our simple calculation as in such extreme cases, general relativistic corrections cannot be ignored. Even the exact calculations for Chandrasekhar mass limit for neutron stars have not been worked out yet. We only have an idea of an upper limit of about $3M_\odot$ and a lower limit - the same as the white dwarf Chandrasekhar mass. Moreover, a more realistic equation of state needs to be considered. Current best estimates of the size of neutron stars puts them at a diameter between 19 to 27 km, which is remarkably accurate given the distance and characteristics.

From what was discussed in type two supernovae, we expect a lot of these considering the

rates of core collapse supernovae - up to a hundred million of them in our own galaxy. Given their extremely small radius, their luminosity is expected to be low (6.1). However, they have a very high temperature too and are expected to shine brightly in the X-ray region of the electromagnetic spectrum. As it turns out, they do - so brightly that they could appreciably ionise the Earth's upper atmosphere. One of the first of these was observed roughly from the constellation Scorpius and thus was named Scorpius X-1.

Using the Wein's displacement law, these are expected to have temperatures of tens of millions of degrees. Using the distance to Scorpius X-1, its luminosity comes out to be a few by 10^{31} W. Once again, using the Stefan-Boltzmann equation one of the first estimates of its radius came out to be 6 km.

One possible source of this temperature could be the supernova that produced it, but at this rate they are expected to cool down by radiating away their energy soon.

A second X-ray source detected was somewhere in the Crab nebula - the remains of the 1054AD supernova, so this seems to fit. But unfortunately, detailed measurements of the position (made possible when the Moon covered the source) showed that a large part of the X-rays are actually coming from the extended nebula, and not from a compact object in its centre.

One possibility - neutron stars could be extremely magnetic, if they've trapped some of the magnetic field from the star that formed them. If they are spinning fast, this magnetic field will whip through the surrounding gas, accelerating charges and producing a very strong ultra-low frequency radio signal. These radio waves won't escape the nebula but they can spread the decaying rotational energy out, heating the gas enough to produce X-rays.

Pulsars

The next set of clues was a totally unexpected one - the discovery of pulsars. They were radio sources pulsing around once a second. It is possible to calculate the maximum rotation period for any body held by gravity - by setting the centrifugal force equal to gravity at the surface. This gives the maximum possible radius for a body of given mass M and spin period P :

$$r = \sqrt[3]{\frac{GMP^2}{4\pi^2}}$$

This gives an upper limit on the size that is much smaller than a white dwarf. This leaves neutron stars as the only possibility.

And sure enough - a pulsar was detected in the centre of the Crab nebula. It was strongly magnetic, and its period was decreasing at a rate that was consistent with the magnetic field carrying away its energy to power the X-ray emission from the rest of the nebula! So pulsars seem to be magnetised neutron stars emitting a spinning beam of radio waves.

Some other pulsars which are not associated with supernova remnants are also observed. These seem to have a normal looking star that wobbles - just like a white dwarf binary. So we seem to be seeing a neutron-star equivalent of the dwarf novae: a star feeding matter via the Roche lobe to its binary companion - in this case, a neutron star. Because the companion is smaller and denser, the radiation comes out at X-ray wavelengths rather than UV wavelengths, giving us an X-ray binary.

Pulsars are not only interesting and helpful in understanding stellar evolution - they also act as extremely accurate clocks, rivalling the world's best atomic clocks.

6.2.8 Black Holes

Neutron stars are the last known forms of stable star. In a prescient paper presented to the Royal Society of London in 1783, John Michell noted that, if a star were sufficiently massive, the escape velocity from its surface would exceed the speed of light and so light would not escape from it.

In classical terms, if the escape velocity from the surface of a star exceeds the speed of light, and the gravitational force of these is so immense that no physical force can prevent the collapse to a physical singularity, then such a star would form a black hole. These properties explain the origin of the term - no radiation can emerge from within the radius r_g and so the object is ‘black’, and at the same time the singularity represents a ‘hole’ in space-time into which matter can collapse but from which it cannot emerge. Here r_g is the Schwarzschild radius of a black hole of mass M , though the coordinate r has a different meaning from the Newtonian definition of distance.

Relativity is often best understood by means of space-time diagrams: diagrams with a couple of spatial coordinates shown horizontally (e.g. x and y) but with time shown vertically. In a diagram like this, a stationary object is a vertical line. The faster something moves, the more slanted the line is.

As nothing can move faster than light, there is a maximum possible angle any motion can take, corresponding to the speed of light. This means that for any point in space and time, you can define a “light cone”, indicating where light emitted at that point could get to. As any real object can only travel at the speed of light or less, this means that our point can only influence things inside this cone, and that if you were at that point in space and time, you can only ever reach regions within this cone.

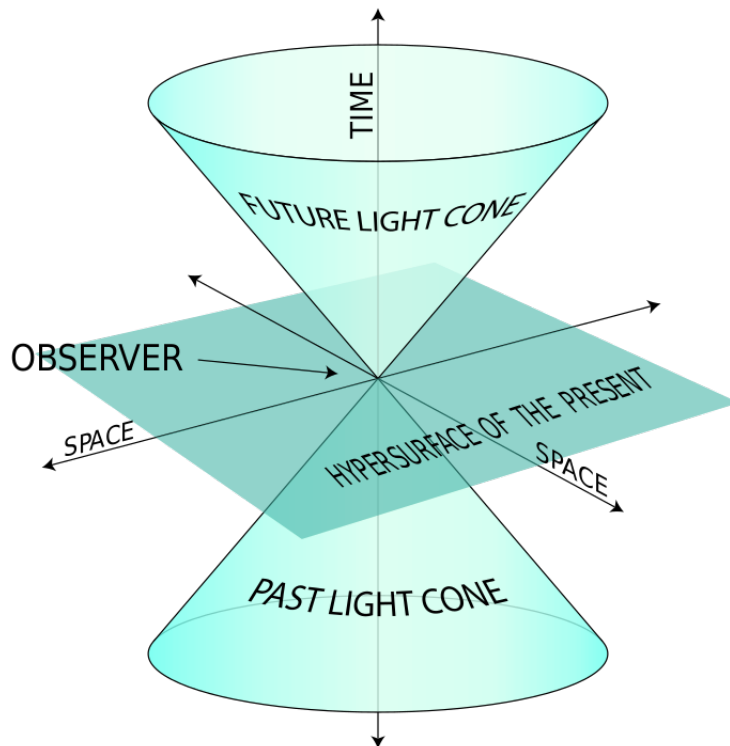


Figure 6.6: Light cone showing 2 axes on xy plane and time along z axis. [5]

Gravity causes these light-cones to tilt over (by distorting space-time). If the light cones are tilted over so much that the far side of the cone is vertical, then staying stationary becomes impossible - you have to move inwards. This is a black hole.

They thus cannot have solid surfaces - matter on the surface would have to move faster than light just to stay put. Everything must thus collapse down to a singularity - a point of huge mass but zero size, and hence infinite density.

While the actual black hole has a radius of zero, it is possible to define an "event horizon" radius - the Schwarzschild radius - the radius at which the edge of the light cone becomes vertical. This radius is given by the equation

$$r_s = \frac{2GM}{c^2}$$

In principle, black holes are formed when a neutron star becomes so massive that its radius is smaller than its event horizon radius. This is possible in a few ways, the first being that the star that collapsed into a neutron star was massive beyond a point to begin with. Some other possible explanations are neutron star mergers (which are a source of gamma ray bursts) and even slow but steady accretion pushing it over the mass limit.

Properties of Black Holes:

Some properties of black holes which can be inferred about black holes through a general relativistic treatment are:

- Dead stars with masses greater than $3M_o$ must be black holes.
- The only properties which isolated black holes can possess are mass, angular momentum and electric charge. This is known as the 'no hair theorem' as they can be completely described by just three properties.
- For a non-rotating black hole, a Schwarzschild black hole, there is a spherical surface about the black hole from which electromagnetic radiation suffers an infinite gravitational redshift, as observed from outside this surface. This surface of infinite redshift has radius

$$r_g = \frac{2GM}{c^2} = 3 \left(\frac{M}{M_o} \right) \text{ km}$$

and is known as the Schwarzschild radius. Radiation with frequency ν_0 emitted at radius r from the black hole suffers a gravitational redshift, so that the frequency of the radiation as observed at an infinite distance from the black hole ν_∞ is

$$\nu_\infty = \nu_0 \left(1 - \frac{2GM}{rc^2} \right)^{1/2} = \nu_0 \left(1 - \frac{r_g}{r} \right)^{1/2}$$

- There is a last stable circular orbit about a Schwarzschild black hole at radius $r = 3r_g$. Within this radius, test particles spiral inevitably into the black hole, contributing to its mass and angular momentum. As will be shown below, the speed of a test particle on the last stable circular orbit of a Schwarzschild black hole is $\nu_\phi = c/2$.
- In the case of black holes with finite angular momentum J , the Kerr black holes, the surface of infinite redshift occurs at radius

$$r_\infty = \frac{GM}{c^2} + \left[\left(\frac{GM}{c^2} \right)^2 - \left(\frac{J}{Mc} \right)^2 \right]^{1/2}$$

There is a maximum angular momentum which a rotating black hole can possess, $J_{max} = GM^2/c$. The radius of the surface of infinite redshift for a maximally rotating black hole then occurs at $r_\infty = GM/c^2 = \frac{1}{2}r_g$, that is, half the Schwarzschild radius of a non-rotating black hole.

- There is a last stable orbit about a Kerr black hole, but now test particles can orbit in either the co-rotating or counter-rotating directions with respect to the angular momentum axis of the black hole. For a maximally rotating Kerr black hole, the last stable circular orbit for co-rotating test particles coincides with r_∞ , that is $r = GM/c^2$, one sixth of the corresponding radius for a non-rotating, Schwarzschild black hole.
- The binding energies of particles on the last stable orbit for Schwarzschild and maximally rotating Kerr black holes, relative to their rest mass energies, are

$$\text{Schwarzschild } \left[1 - \sqrt{\frac{8}{9}} \right] \quad \text{Kerr } \left[1 - \sqrt{\frac{1}{3}} \right]$$

corresponding to 5.72% and 42.3% of their rest mass energies, respectively. A fraction of the rotational energy of a rotating black hole can also be made available to the external Universe. In terms of the rest-mass energy of the black hole, this fraction is

$$1 - 2^{-1/2} \{ 1 + [1 - (J/J_{max})^2]^{1/2} \}^{1/2}$$

amounting to 29% for a maximally rotating Kerr black hole, $J = J_{max}$.

6.3 Active Galactic Nuclei

Some of the initially proposed ways of trying to observe black holes were by observing their gravitational influence of nearby stars. One example is Cygnus X-1 - a binary system where the 'dark' star has 10-20 times the mass of the sun, which eliminates degenerate stars and leaves black holes as the only explanation. Galactic centres also seem to be good candidates for this as they contain lots of stars in a small area, and when observed, most galaxies seem to have a supermassive black hole at their centre. In the case of our own galaxy, the supermassive black hole is estimated to have a mass of about four million times the mass of our sun.

Virtually all galaxies seem to have big black holes in their centres, and the mass of the black hole correlates remarkably tightly with the mass of the central bulge of the galaxy. This is presumably telling us that in some way the formation and evolution of the black hole and its surrounding galaxy are tightly coupled. The biggest black holes are in the centres of giant elliptical galaxies.

A tiny fraction of these galactic centre black holes are incredibly bright and are called active galactic nuclei (AGNs). Some of the brightest, which also emit radio jets, are called quasars. They shine by tearing apart matter falling in towards them, and hence liberating some fraction of their gravitational potential energy as heat before the matter disappears into the event horizon.

Most galaxies, however, do not have anything this bright in their centres. In some cases this is because the central black hole is obscured by dust, but in most cases it is probably because the black hole has already eaten everything close to it, and hence cannot shine any more.

Thus it is commonly believed that galaxy collisions provide material to the galactic nuclei, causing them to light up. Unfortunately, galaxies in the middle of collisions seem to be no more

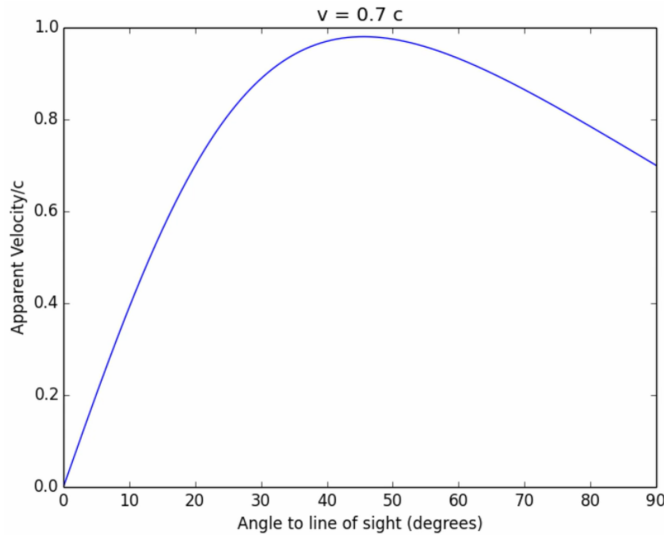


Figure 6.7: Superluminal motion at $v = 0.7c$

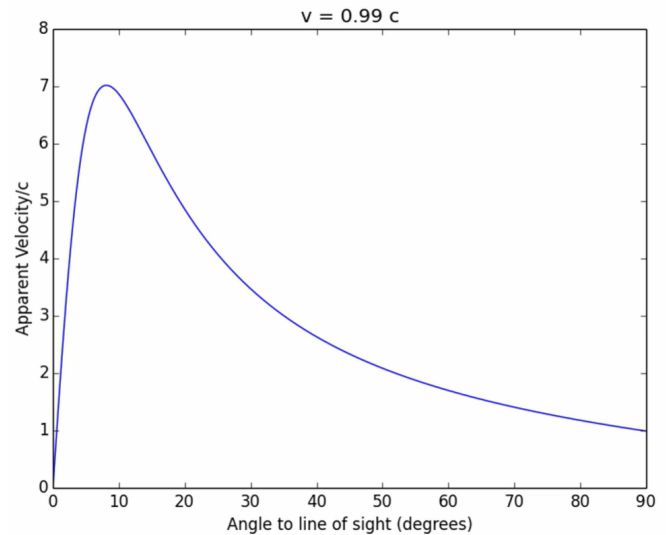


Figure 6.8: Superluminal motion at $v = 0.99c$. [6]

likely than other galaxies to host an active nucleus - this is a puzzle.

One of the strangest types of active galaxies are blazars (not to be confused with quasars - they are the same thing, just oriented differently with respect to earth). In these objects, a jet of material is travelling close to our line of sight at very near the speed of light. Blobs in these jets appear to move away from the nucleus at faster than the speed of light - a phenomenon called superluminal motion. However, this is just an optical illusion.

If we observe the blob of material from the jet to have travelled a distance of Δr in time Δt , then its apparent velocity will be $v = \Delta r / \Delta t$. However, two factors need to be considered here. Firstly, the observed motion will be the sideways motion from the jet. If the angle to the line of sight is θ , the $\Delta r_{obs} = r \sin \theta$ where r is the actual distance travelled. Secondly, the time observed by observers on earth will be different to the time observed from the quasar's perspective. This is because the light coming from the blob after Δt_{obs} will have to travel a shorter distance as the source of this light, the blob, has moved towards us. Thus $\Delta t_{obs} = (ct - r \cos \theta) / c$. Using the substitutions $\beta = v/c$ and $r = vt$,

$$v_{obs} = \frac{\beta \sin \theta}{1 - \beta \cos \theta}$$

Thus using this expression, the graphs in Figures 6.3, it can be seen that at particular values of θ for given high value β , the observed velocity can easily cross c .

Bibliography

- [1] *High energy astrophysics. Vol. 1: Particles, photons and their detection.* 1992
- [2] *The high energy universe: ultra-high energy events in astrophysics and cosmology.* 2010.
- [3] European Southern Observatory. <https://www.eso.org/>
- [4] National Aeronautics and Space Administration <https://www.nasa.gov/>
- [5] 2007-05-07 07:39 K. Aainsqatsi 481×491× (105860 bytes) Source = self-made Information—Description = SVG version of http://en.wikipedia.org/wiki/Image:World_line.png
- [6] EdX Course: Astrophysics: The Violent Universe from Australian National University <https://courses.edx.org/courses/course-v1:ANUx+ANU-ASTRO3x+1T2016/course/>